1-2-2 ENAMI (1992): INFORME GEOLOGICO FINAL PROYECTO DE ESTUDIOS PROGRESO PERTENENCIAS PROGRESO 1-211 COPIAPO, III REGION, CHILE

A geological & geochemical survey was carried out in the Progreso 1-211 mining field owned by ENAMI; in addition to studying the possibility of the generation of copper deposits within the Punta de Cobre formation in the area, as a subsequent step it was suggested that geoelectric prospecting be carried out, and drilling survey conducted for the anomalies thus obtained.

A summary of the results of this survey follows.

1. The geology of the area and its environs is comprised of lower Cretaceous volcanic and sedimentary rocks, intrusive rocks thought to have been active from the mid-Cretaceous to early Tertiary Periods, and unconsolidated sediment of the Pleistocene and Holocene Periods.
2. The volcanic rocks and sedimentary rocks of the lower Cretaceous period are classified, from the bottom, into the Punta del Cobre, Abundancia, Nantoco and Bandurrias formations.
   Of these, distributed within the survey area are the Punta del Cobre and Abundancia formation.
3. The Punta del Cobre formation is distributed in the foothills on both the east and west sides of the Copiapo River, along an anticlinal axis in a NE-SW direction. The formation may be divided into a lower (kpcli) and an upper (kpcls) strata. The lower stratum is made up of mainly andesitic lava, and the nether limit of the stratum is unascertained. The upper stratum has a depth of 60-120 m, and is made up of andesitic lava, andesitic tuff breccia, lapilli tuff and tuff volcanic rocks, intercalated with sedimentary rocks, such as slate, sandstone, calcareous sandstone, limestone, etc.
   Within the area, albitized meta-andesite of the upper stratum are exposed in parts, but mostly they are covered by a Quaternary stratum.
4. The Abundancia formation covers the Punta del Cobre formation, and is distributed in its east, south and southwest parts. The formation is divided into three layers, from the bottom, kad, kau and kam. The kad layer is a stratified limestone-prominent stratum, the kau layer a weakly-stratified to massive limestone stratum sandwiched with trachytic tuff, and the kam bed is made up of skarn accompanying mineralization.
   These formations are in conformity, showing a strike in a NNE to NE direction and forming an anticlinorium with an axis in the same direction. The area is located on the western wing of the anticlinorium, and with the trachytic tuff of the kau layer as the key stratum it is possible to suppose the location of the upper layer of the Punta del Cobre formation.
5. The intrusive rocks are made up of granites of the Andes batholith distributed widely on the western side of the Copiapo River, and acidic to basic dikes penetrating them.
6. The above-mentioned rocks are controlled by a folding structure with a NE-SW axis and a NW-SE, N-S fracture structure.
   On the west side of the Copiapo River, this tendency is strong, and the NW-SE, N-S lineament is

prominent. On the east side of the Copiapo River each stratum has a gentle easterly incline, but in the NE part where the survey area is located the folding structure and thrust fault accompanying it, are developed.

7. The ore deposits in the area and its environs are classified into three as shown below, and are generated controlled by the folding structure in the NE-SW direction and the NW-SE, N-S fracture structure.

   a) Manto type, breccia type and vein type ore deposits with the Punta del Cobre formation as the country rock. Made up of chalcopyrite - pyrite - magnetite - hematite ores.

   b) Manto type ore deposits with the garnet skarn and hornfels of the Abundancia formation as the country rock. Made up of gold-bearing oxidized copper - chalcopyrite ores.

   c) Gold-bearing iron ore vein-type deposits within the Andes batholith as the country rock.

   Of these, a) is of economic value, and there are mines in operation on both east and west sides of the Copiapo River.

8. In the Progreso area, the southeast and northern parts are selected as fields for exploration. The southeast part conceals the Punta del Cobre stratum, which is a horizon for manto-type ore deposits, and a geochemical investigation of the rocks in the kau layer, the upper layer distributed on the surface, produced values of Cu:205-1660ppm, Au:<50ppb, Ag:6.3-20ppm. The Punta del Cobre stratum is also concealed in the northern part, covered by alluvium; in the skarn in the upper kam layer, mineral indications of mainly pyrite have been found, and in a geochemical rock survey of the outcrops values of Cu:35-585 ppm have been obtained.

9. It was suggested that electrical prospecting be carried out in the areas given above, and drilling survey conducted for the anomalies thus obtained.

1-2-3 ENAMI (1993): ESTUDIO GEOFISCO MEDIANTE CSAMT Y POLARIZACION INDUCIDA ESPECIAL PROYECTO PROGRESO, COPIAPO III REGION SECTOR PAN, PROGRESO SUR INTERMEDIO Y PROGRESOSUR

As a result of CSAMT and SIP surveys carried out in the three regions PAN, SUR INTERMEDIO and SUR within the Progreso 1-211 mining field, CSAMT and SIP anomalies were found to overlap in the border area between the SUR region and the SUR INTERMEDIO region, and this was chosen as having a high mineralization potential.

1-2-4 ENAMI (1993): ESTUDIO GEOFISCO MEDIANTE CSAMT Y POLARIZACION INDUCIDA ESPECTRAL PROYECTO PROGRESO, COPIAPO III REGION PROGRESO NORTE

As a result of CSAMT and SIP surveys carried out in the Northern region within the Progreso 1-211 mining field, a CSAMT low resistitivity band was found to exist in lens form in the level of the Punta del Cobre formation in the west-central part of the area. Since this overlaps with a SIP anomaly, the site was chosen as having a high mineralization potential.

However, it was suggested that prior to a drilling survey, the SIP survey should be conducted on lines P-1,3,4,5,7, in addition to P-2; and in order to carry out a detailed survey of the low resistitivity band in the horizon of the Punta del Cobre formation, it was suggested that a TEM(transient electromagnetic method) be performed on lines P-1 to 5 with measuring points at 50m interval.

A comprehensive analysis of these physical survey data and the geological conditions is suggested, followed by the drawing-up of a boring schedule.

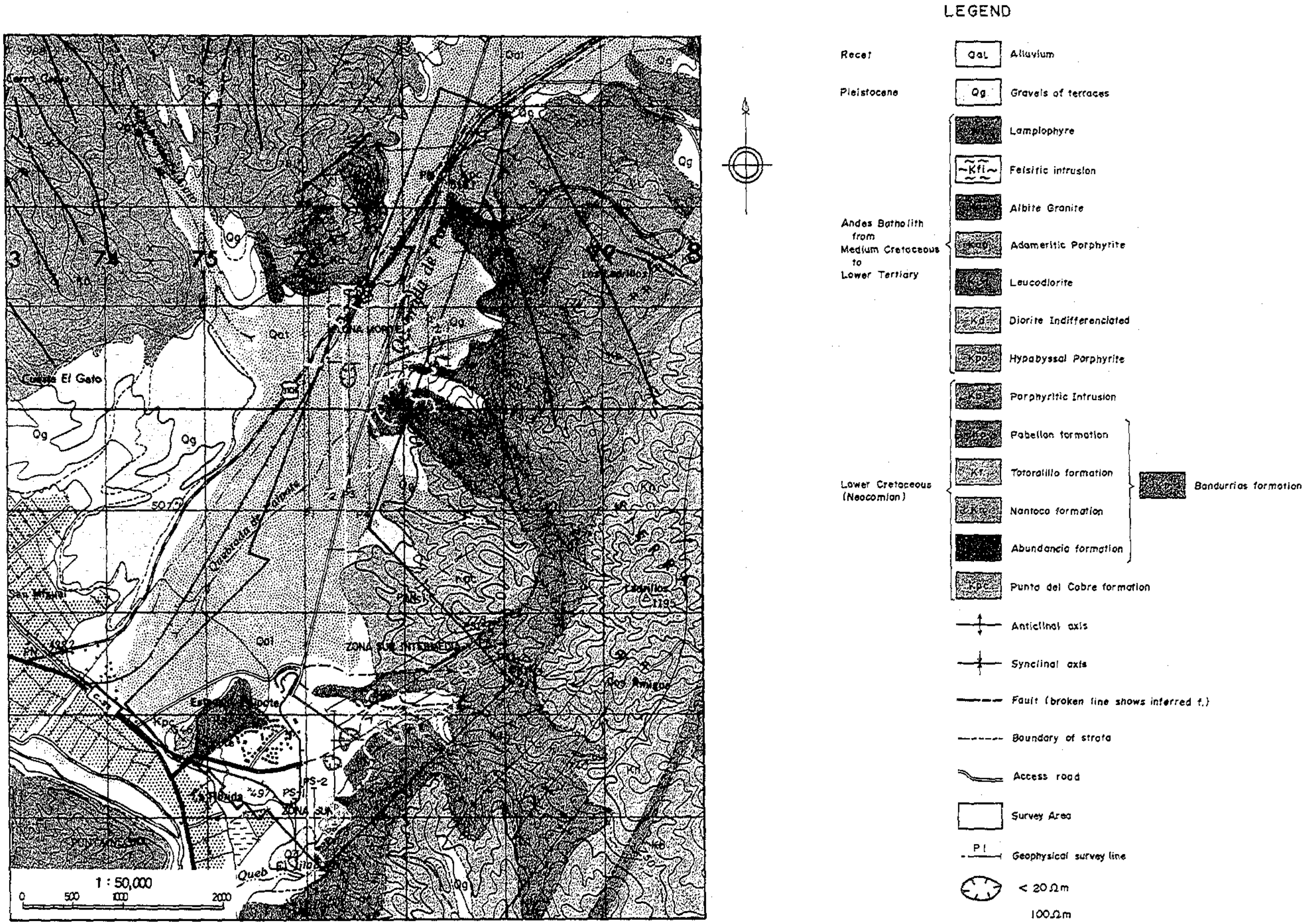

Fig.II-1-2 Synthetic map of the Progreso area

CHAPTER 2 DRILLING SURVEY IN THE VERAGUAS AREA

2-1 Purpose

The purpose of this survey was to discover the existence of copper ore deposits through core-boring in the area in which, from an overall analysis of existing survey data, it may be considered highly possible for copper ore deposits to exist.

According to existing survey data, low resistivity anomalies by CSAMT have been confirmed in the areas of alteration rock of the Cerro Veraguas and the Sierra Overa, and it is considered there is a strong possibility of copper ore deposits lying beneath these mountains. As is shown in Fig.II-2-1, the drilling sites were chosen with these CSAMT anomalies and the alteration zones in mind.

The position coordinates, direction, inclination and depth of each boring hole are shown in Table II-2-1.

Table II-2-1 Contents of Drilling

Drill Hole	N	E	H(m)	Dir.	Incli.	Depth
MJCV-1	7,145,750.00	400,850.00	1,830.00	N90° W	-65	402.0m
MJCV-2	7,145,750.00	401,400.00	1,800.00	N90° W	-60	350.0m
MJCV-3	7,144,750.00	400,850.00	1,717.32	---	-90	401.0m
MJCV-4	7,143,220.00	399,180.00	1,459.98	N90° W	-35	500.0m
MJCV-5	7,142.000.00	396,400.00	1,550,00	N90° W	-55	400.0m
Total						2,053.0m

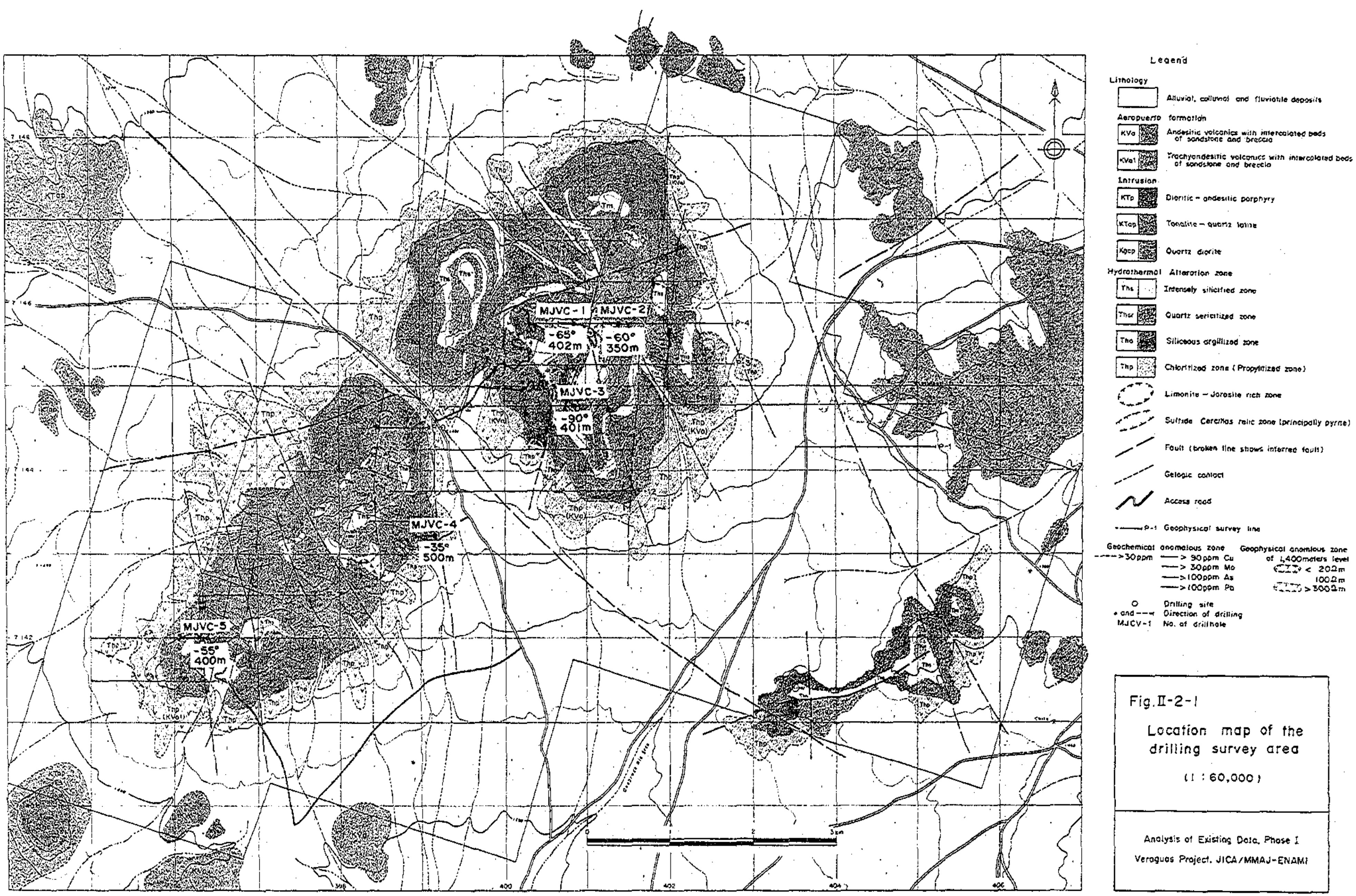

Fig.II-2-1

Location map of the drilling survey area

(1 : 60,000)

Analysis of Existing Data, Phase I

Veraguas Project, JICA/MMAJ-ENAMI

Table II-2-2 Equipments of drilling

ITEM	SPEC.	TOTAL	1st	2nd	3rd	REMARKS
DRILLING MACHINE		3	LY-44 (1)	LY-44 (2)	LY-38	set
DRILLING PUMP	BEAN ROYAL 434	3	1	1	1	set
DRILL RODS	HXWL	235	85	85	65	@ 3.05m/rod
	NXWL	430	170	140	120	@ 3.05m/rod
	BXWL	310	170	140		@ 3.05m/rod
INNER TUBE ASSEMBLY	HXWL	9	3	3	3	set
	NXWL	9	3	3	3	set
	BXWL	9	3	3	3	set
CORE BARREL ASSEMBLY	HXWL	9	3	3	3	set
	NXWL	9	3	3	3	set
	BXWL	9	3	3	3	set
CASING	HWCP	201	67	67	67	@ 3.05m/rod
	NXCP	300	100	100	100	@ 3.05m/rod
	BXCP	0				@ 3.05m/rod
DRILLING DEPTH	MJCV-1	402.0		402.0		m
	MJCV-2	350.0			350.0	m
	MJCV-3	401.0		401.0		m
	MJCV-4	500.0	500.0			m
	MJCV-5	400.0	400.0			m

Table II-2-3 Articles of consumption

ITEM	SPEC.	TOTAL	MJCV-1	MJCV-2	MJCV-3	MJCV-4	MJCV-5
TRICON BIT		3	1			1	1
DIAMOND BIT	HX	16	2	2	5	5	2
	NX	10	2	2	2	2	2
	BX	3	1				2
REAMING SHELL	HX	6	1	1	2	1	1
	NX	5	1	1	1	1	1
	BX	2	1				1
CASING SHOE	HX	5	1	1	1	1	1
	NX	5	1	1	1	1	1
	BX	0					
CEMENT	bag	22				12	10
BENTONITE	bag	384	132	79	100	36	37
REPONITE	kg	198	88	22	22	22	44
C.M.C.	kg	484	132	44	154	44	110
POLYMER	l	620	40	120	140	160	160
CAUST.SODA	kg	400	50	100		50	200
GYPSUM	bag	6			6		
GASOLINE	l	24130	4490	3560	4540	6450	5090

Table Ⅱ-2-4 Program of drilling

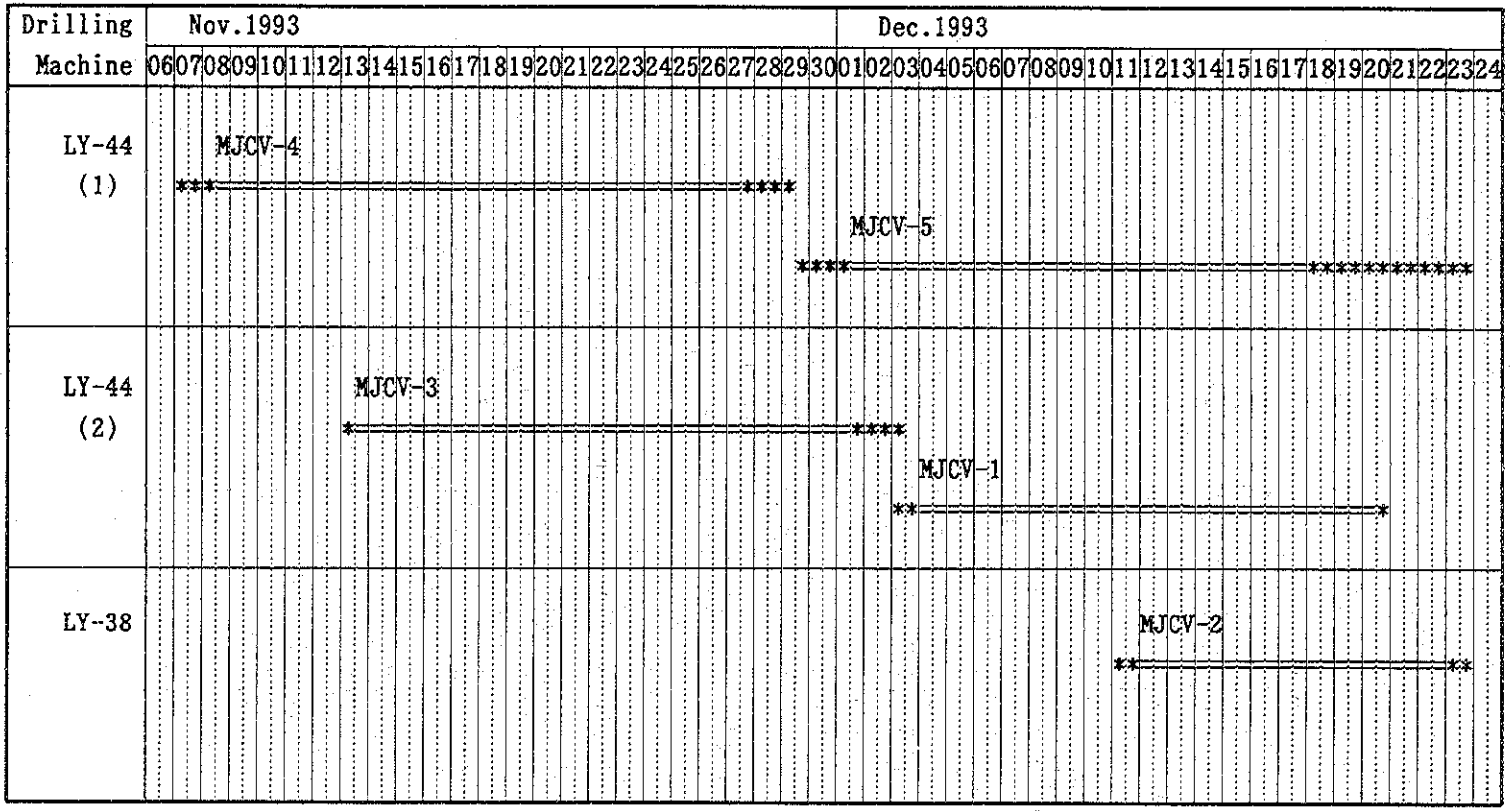

====== DRILLING ****** MOBILIZATION & DEMOBILIZATION

Table II-2-5 Summary of drilling activity (1)

MJCV-1	PERIOD	TOTAL TURNS	WORKING TURNS	DAY OFF TURNS	TURN *WORKER	DAYS
MOBILIZATION	12/03	2	2	0	8	1.0
DRILLING	12/04-20	33	33	0	132	16.5
DEMOBILIZATION	12/20	1	1	0	4	0.5
TOTAL	12/03-12/20	36	36	0	144	18.0
DEPTH PLANNED	400.00	(m)	DRILLING	24.36 (m/drilling day)		
DEPTH DRILLED	402.00	(m)	SPEED	22.33 (m/total working day)		
OVER BURDEN	0.00	(m)	CASING	11.00 HWCP(m)		
CORE LENGTH	366.82	(m)		115.40 NXCP(m)		
CORE RECOVERRY	91.25	(%)				

MJCV-2	PERIOD	TOTAL TURNS	WORKING TURNS	DAY OFF TURNS	TURN *WORKER	DAYS
MOBILIZATION	12/11	2	1	1	4	1.0
DRILLING	12/12-22	22	22	0	88	11.0
DEMOBILIZATION	12/23	2	2	0	8	1.0
TOTAL	12/11-12/23	26	25	1	100	13.0
DEPTH PLANNED	350.00	(m)	DRILLING	31.82 (m/drilling day)		
DEPTH DRILLED	350.00	(m)	SPEED	26.92 (m/total working day)		
OVER BURDEN	0.00	(m)	CASING	1.65 HWCP(m)		
CORE LENGTH	312.92	(m)		103.50 NXCP(m)		
CORE RECOVERRY	89.41	(%)				

MJCV-3	PERIOD	TOTAL TURNS	WORKING TURNS	DAY OFF TURNS	TURN *WORKER	DAYS
MOBILIZATION	11/13	1	1	0	4	0.5
DRILLING	11/13-12/01	36	36	0	144	18.0
DEMOBILIZATION	12/01-03	3	2	1	8	1.5
TOTAL	11/13-12/03	40	39	1	156	20.0
DEPTH PLANNED	400.00	(m)	DRILLING	22.28 (m/drilling day)		
DEPTH DRILLED	401.00	(m)	SPEED	20.05 (m/total working day)		
OVER BURDEN	0.00	(m)	CASING	6.20 HWCP(m)		
CORE LENGTH	341.11	(m)		193.80 NXCP(m)		
CORE RECOVERRY	85.06	(%)				

Table II-2-5 Summary of drilling activity (2)

MJCV-4	PERIOD	TOTAL TURNS	WORKING TURNS	DAY OFF TURNS	TURN *WORKER	DAYS
MOBILIZATION	11/07-08	3	2	1	8	1.5
DRILLING	11/08-27	38	38	0	152	19.0
DEMOBILIZATION	11/27-29	4	4	0	16	2.0
TOTAL	11/07-29	45	44	1	176	22.5
DEPTH PLANNED	500.00 (m)		DRILLING	26.32 (m/drilling day)		
DEPTH DRILLED	500.00 (m)		SPEED	22.22 (m/total working day)		
OVER BURDEN	1.70 (m)		CASING	1.70 HWCP(m)		
CORE LENGTH	446.54 (m)			195.90 NXCP(m)		
CORE RECOVERRY	89.61 (%)					

MJCV-5	PERIOD	TOTAL TURNS	WORKING TURNS	DAY OFF TURNS	TURN *WORKER	DAYS
MOBILIZATION	11/29-12/01	4	3	1	12	2.0
DRILLING	12/01-17	33	33	0	132	16.5
DEMOBILIZATION	12/18-23	12	6	6	24	6.0
TOTAL	11/29-12/23	49	42	7	168	24.5
DEPTH PLANNED	400.00 (m)		DRILLING	24.24 (m/drilling day)		
DEPTH DRILLED	400.00 (m)		SPEED	16.33 (m/total working day)		
OVER BURDEN	1.45 (m)		CASING	3.05 HWCP(m)		
CORE LENGTH	366.10 (m)			167.95 NXCP(m)		
CORE RECOVERRY	91.86 (%)					

TOTAL	PERIOD	TOTAL TURNS	WORKING TURNS	DAY OFF TURNS	TURN *WORKER	DAYS
MOBILIZATION	11/07-	12	9	3	36	6.0
DRILLING	11/08-12/22	162	162	0	648	81.0
DEMOBILIZATION	-12/23	22	15	7	60	11.0
TOTAL	11/07-12/23	196	186	10	744	98.0
DEPTH PLANNED	2050.00 (m)		DRILLING	25.35 (m/drilling day)		
DEPTH DRILLED	2053.00 (m)		SPEED	20.95 (m/total working day)		
OVER BURDEN	3.15 (m)		CASING	23.60 HWCP(m)		
CORE LENGTH	1833.49 (m)			776.55 NXCP(m)		
CORE RECOVERRY	89.45 (%)					

2-2 Operation Condition

The site investigation period for the drilling survey was from 29th October 1993 to 31st December 1993. Of that time the period of drilling work was from 7th November 1993 to 23rd December 1993. The drilling machines used for the work and consumption supplies are shown in Table II-2-2 and Table II-2-3 respectively; drilling work charts for each boring hole and the drilling progress charts are shown in Table II-2-4 and Table II-2-5.

Drilling operations were carried out as shown in the drilling progress chart, with size of HX, NX, BX; and a core recovery rate of 89.45% including surface soil and talus was achieved. Drilling efficiency varied greatly depending on the geological conditions, due in particular to the crumbling of holes in clay areas and inundation in and around the fracture zone. The average drilling efficiency for individual holes was 16.33 - 26.92 m/total working day, the overall average being 20.95 m/total working day.

2-3 Result of Survey

As stated above, the core recovery rate by drilling was good. Color photographs were taken of the cores collected, and visual appraisal of the cores was made; samples were also taken for ore analysis. The remaining cores after the samples had been taken were placed in 4 m lengths in lidded wooden boxes and stored in a local warehouse. The appendix A shows the columnar boring section on a scale of 1:200 drawn up from the visual appraisal of the boring cores.

For the ore analysis, each core was split in half using a diamond cutter, and analytic samples taken every metre. The results of the analysis are listed in the appendix B.

For observation of the boring cores, samples of ore and rock deemed necessary were taken and subjected to polished thin-section observation and X-ray diffraction, and this was used as a reference in the analysis of the boring columnar section and the boring profile. Table II-2-6 shows the results of the polished thin-section observation; and Table II-2-7 shows the results of the X-ray diffraction analysis.

The geological state of each boring hole and the state of mineralization alteration, will be explained fully in the section on each hole.

2-3-1 MJCV-1

1. Outline

(1) Reasons for drilling

This hole is located 400 m west of the peak of the Cerro Veraguas. From the fact that in the zone of hydrothermal alteration around the hole the breccia structure accompanied by hematite is developed and is thought to have been a passage for ore solution, and that a CSAMT (ENAMI, 1993) found it was in a medium resistivity band of 100-300 ohm.m, the existence of underlying mineral indications may be expected.

(2) Summary of results

The hole is made up of andesitic volcanics and porphyry that have undergone hydrothermal alteration. The hydrothermal alteration can be divided into intensely silicified, quartz-sericitized, siliceous argillized and chloritized zones. The porphyry is disseminated with pyrite, and minute amounts of copper minerals, such as chalcopyrite, chalcocite, covelline etc., may be observed. In particular, there is a tendency for the copper grade to be high around the border between the porphyry and the andesitic volcanics.

The position coordinates of the hole and drilling details are as given below:

Coordinates:	7,145,750.00N	400,850.00E	1,830.00m above sea level
Drilling details:	Direction N90°W	Inclination -65°	Depth 402.00m

2. Geology

(1) Litho-Units

Depth	Original rock	Alteration Zone	Mineralization
0.00- 72.05m	andesite lava	intense silicified & quartz sericitized	hematite dissemination
72.05-123.75m	andesite autobrecciated lava	siliceous argillized	hematite dissemination
123.75-148.85m	Ditto(fracture zone)	siliceous argillized	jarosite,limonite,hematite prominent
148.85-196.40m	andesite autobrecciated lava	siliceous argillized	jarosite,limonite,hematite dominant
187.40-292.20m	porphyry	siliceous argillized	pyrite dissemination
292.20-318.00m	andesite autobrecciated lava	siliceous argillized	jarosite,limonite,hematite dominant
318.00-333.00m	fracture zone	siliceous argillized	jarosite,limonite,hematite dominant
333.00-353.50m	andesite autobrecciated lava	siliceous argillized	hematite dissemination
353.50-400.00m	porphyry	propylite, potassium addition in parts	pyrite dissemination

(2) Alteration

The intensely silicified and quartz-sericitized zones cover the peak area to a depth of approximately 70m. The border between the two zones is not clearly defined. Underlying these, a siliceous argillized zone of mainly kaolinite extends for a depth of approximately 300m. In and around the NW-SE, NE-SW fracture zone the kaolinization is dominant, and is accompanied by conspicuous concentrations of jarosite, limonite and hematite. In the lower part of the siliceous argillized zone, chloritization becomes stronger, and shifts gradually into the chloritized zone.

(3) Mineralization

Hematite dissemination and/or film occurs in the intensely silicified, quartz-sericitized and siliceous argillized zones with andesite as the original rock. Pyrite dissemination and/or film occurs in the siliceous argillized and chloritized zones with porphyry as the original rock, larger amounts being contained in the latter. Under the microscope, chalcopyrite, chalcocite and covelline are found associated with pyrite.

3. Results of Ore Analysis

Places where the grade of T.Cu is 500ppm or above are shown below as the range of mineralization.

There is a tendency for the copper grade to be higher near the borders of the andesitic lava and porphyry of the siliceous argillized and chloritized zones.

Depth m - m	Range m	T.Cu ppm	S.Cu ppm	Mo ppm	Au ppm	Ag ppm	T.Fe %	Original Rock	Alteration Zone
194 195	1	820	520	8	<0.04	0.7	4.38	Porphyry	Siliceous argillized zone
208 209	1	910	590	9	<0.04	0.6	4.00	Porphyry	Siliceous argillized zone
291 292	1	540	400	6	<0.04	0.5	3.35	Porphyry/Andesite	Siliceous argillized zone
352 354	2	670	375	22	<0.04	0.8	4.54	Andesite/Porphyry	Chloritized zone

4. Comparison with CSAMT results

From the fact that the siliceous argillized zone is in the medium resistivity band of 100-300 ohm.m corresponds to the siliceous argillized zone.

2-3-2 MJCV-2

1. Outline

(1) Reasons for drilling

This hole is located 150m east of the peak of the Cerro Veraguas, 550m east of MJCV-1. From the fact that the low-to-medium resistivity band of 0-300 ohm.m by CSAMT (ENAMI, 1993) is widely distributed, some mineral indications may be expected.

(2) Summary of results

The hole is made up of andesitic volcanics and porphyry that have undergone hydrothermal alteration. The hydrothermal alteration belongs to the siliceous argillized zone, but at 235.30m and below there are continuous fracture zones with intense kaolinization, and concentrations of jarosite, limonite and hematite. The porphyry is disseminated with pyrite, and in parts covelline and chalcocite are found in film and disseminate form. In particular, there is a tendency for the copper grade to be high in the fracture zone developed within the porphyry.

The position coordinates of the hole and drilling details are as given below:

Coordinates:	7,145,750.00N	401,400.00E	1,800.00m above sea level
Drilling details:	Direction N90°W	Inclination -60°	Depth 350.00m

2. Geology

(1) Litho-Units

Depth	Original rock	Alteration Zone	Mineralization

0.00- 57.10m	andesitic lava	siliceous argillized	hematite dissemination
57.10- 91.80m	andesitic pyroclastic rock	siliceous argillized	hematite dissemination
91.80-112.10m	andesitic lava	siliceous argillized	hematite dissemination
112.10-132.00m	fracture zone	siliceous argillized	jarosite,limonite,hematite prominent
132.00-158.20m	andesitic autobrecciated lava	siliceous argillized	hematite dissemination
158.20-235.30m	dioritic porphyry		pyrite dissemination
235.30-350.00m	fracture zone	siliceous argillized	jarosite,limonite,hematite prominent

(2) Alteration

The siliceous argillized zone lies to a depth of approximately 300m from the surface. It is expected that in the lower parts this zone shifts into a chloritized zone, but no evidence of this is seen at this hole. In and around the NW-SE, NE-SW fracture zone the kaolinization is dominant and is accompanied by concentrations of jarosite, limonite and hematite.

(3) Mineralization

Pyrite disseminate and/or film occurs in the dioritic porphyry. Between 158.00m-165.00m covelline accompanies pyrite, and between 206.75-207.15m sphalerite and galena are seen in film. In addition, under the microscope chalcopyrite and pyrrhotite accompanies pyrite.

3. Results of Ore Analysis

Places where the grade of T.Cu was 500ppm or above are shown below as the range of mineralization.

There is a tendency for the copper grade to be higher in the fracture zone generated in the siliceous argillized porphyry.

Depth m - m	Range m	T.Cu ppm	S.Cu ppm	Mo ppm	Au ppm	Ag ppm	T.Fe %	Original Rock	Alteration Zone
160 161	1	744	305	6	<0.04	1.0	7.04	Diolitic porphyry	Siliceous argillized zone
237 239	2	897	240	18	<0.04	0.9	4.52	Ditto(Fracture zone)	Siliceous argillized zone
245 246	1	750	45	11	<0.04	<0.4	5.84	Ditto(Fracture zone)	Siliceous argillized zone
291 293	2	1100	376	7	<0.04	0.5	3.24	Ditto(Fracture zone)	Siliceous argillized zone
296 297	1	502	256	5	<0.04	0.8	4.40	Ditto(Fracture zone)	Siliceous argillized zone

4. Comparison with CSAMT results

The siliceous argillized zone is in a low-to-medium resistivity band of 0-300 ohm.m. From the fact that the fracture zone with marked argillization and concentrations of jarosite, limonite and hematite is in the 0-100 ohm.m range, and the dioritic porphyry disseminated with pyrite that has undergone weak kaolinization is the 100-300 ohm.m range, it may be considered that the resistivity values are affected by the degree of argillization and the presence of sulfide.

2-3-3 MJCV-3

1. Outline

(1) Reasons for boring

This hole is located 1,000m south of MJCV-1, on the southern hillside of the Cerro Veraguas. From the fact that the zone of hydrothermal alteration around this hole corresponds to the low resistivity range of 0-100 ohm.m by CSAMT (ENAMI, 1993), some mineral indications may be expected.

(2) Summary of results

The hole is made up of andesitic volcanics and porphyry that have undergone hydrothermal alteration. The hydrothermal alteration can be divided into intensely silicified, siliceous argillized and chloritized zones in descending order. The porphyry belonging to the chloritized zone is disseminated with pyrite, and in parts minute traces of copper minerals - chalcopyrite, chalcocite and covelline - can be found. In particular, there is a tendency for the copper grade to be high around the border with the andesitic volcanics.

The position coordinates of the hole and drilling details are as given below:

Coordinates:	7,144,750.00N	400,850.00E	1,717.32m above sea level
Drilling details:	Direction ---	Inclination -90°	Depth 401.00m

2. Geology

(1) Litho-Units

Depth	Original rock	Alteration Zone	Mineralization
0.00- 68.50m	andesitic lava	intensely silicified	hematite dissemination
68.50- 92.50m	andesitic lava	siliceous argillized	hematite dissemination
92.50-123.20m	fracture zone	siliceous argillized	jarosite,limonite,hematite prominent
123.20-207.00m	porphyry	siliceous argillized	hematite dissemination
207.00-215.50m	andesitic autobrecciated lava	siliceous argillized	hematite dissemination
215.50-229.50m	porphyry	siliceous argillized	hematite dissemination
229.50-256.20m	andesitic autobrecciated lava	siliceous argillized	hematite dissemination
256.20-279.60m	fracture zone	siliceous argillized	jarosite,limonite,hematite prominent
279.60-317.70m	andesitic autobrecciated lava	siliceous argillized	hematite dissemination
317.70-349.00m	porphyry	propylite	pyrite dissemination
349.00-368.35m	andesitic autobrecciated lava	propylite	hematite dissemination
368.35-401.00m	porphyry	propylite	pyrite dissemination

(2) Alteration

The intensely silicified zone covers the mountainside to a depth of approximately 70m. Underlying this, a siliceous argillized zone of mainly kaolinite extends for a depth of 200-300m. In and around the NW-SE, NE-SW fracture zone the kaolinite argillization is dominant, and is accompanied by concentrations of jarosite, limonite and hematite. In the lower part of the siliceous argillized zone, chloritization becomes stronger, and shifts gradually into the chloritized zone.

(3) Mineralization

The pyrite dissemination in porphyry that has undergone chloritization below 317.70m is conspicuous. Chalcocite film and/or dissemination occurs, in addition to which under the microscope chalcopyrite and covelline accompanies pyrite, between 331.90m-349.00m and between 368.10m-371.20m.

3. Results of Ore Analysis

Places where the grade of T.Cu was 500ppm or above are shown below as the range of mineralization.

There is a tendency for the copper grade to be higher in the porphyry of the chloritized zone, and particularly in the area close to the border with the andesitic volcanics.

Depth m - m	Range m	T.Cu ppm	S.Cu ppm	Mo ppm	Au ppm	Ag ppm	T.Fe %	Original Rock	Alteration Zone
305 307	2	76	17	203	<0.04	<0.4	6.01	Andesite	Siliceous argillized zone
315 316	1	1100	804	69	<0.04	<0.4	2.58	Andesite/Porphyry	Siliceous argillized zone
321 323	2	505	252	21	<0.04	<0.4	3.23	Porphyry	Chloritized zone
326 327	1	80	53	213	<0.04	<0.4	3.15	Porphyry	Chloritized zone
332 333	1	770	396	36	<0.04	<0.4	2.68	Porphyry	Chloritized zone
336 338	2	560	198	70	<0.04	<0.4	2.36	Porphyry	Chloritized zone
346 349	3	1587	511	13	<0.04	<0.4	1.48	Porphyry/Andesite	Chloritized zone
358 359	1	86	13	206	<0.04	<0.4	4.00	Andesite	Chloritized zone
368 369	1	7000	1263	24	<0.04	<0.4	7.42	Andesite/Porphyry	Chloritized zone
369 370	1	2300	954	36	<0.04	<0.4	6.48	Porphyry	Chloritized zone
377 378	1	948	86	12	<0.04	<0.4	6.24	Porphyry	Chloritized zone
389 390	1	1400	443	16	0.07	<0.4	6.80	Porphyry	Chloritized zone
395 396	1	700	138	16	<0.04	1.3	10.24	Porphyry	Chloritized zone

4. Comparison with CSAMT results

The intensely silicified zone to a depth of 68.50m from the surface corresponds to a high resistivity band of >300 ohm.m. From the fact that the high resistivity band displays a configuration that hangs down deep on both the east and west sides of the hole, it may be expected to develop toward the lower part of the silicified zone. The siliceous argillized zone is in a low-to-medium resistivity band of 0-300 ohm.m. Within this, the markedly argillized fracture zone with concentrations of jarosite, limonite and hematite is in the range 0-100 ohm.m. The pyrite-disseminated porphyry in the chloritized zone below 317.70m is also in the range 0-100 ohm.m, but this may be considered to be due to the influence of the alteration above it.

2-3-4 MJCV-4

1. Outline

(1) Reasons for drilling

This hole is located on the eastern foot of the Sierra Overa, approximately 1,500 m southeast of the San Juan Mine.

Since the San Juan deposits and geochemical anomalies in Cu and Mo distribute in the vicinity of the hole, and from the fact of low-to-medium resistivity band range of 0-300 ohm.m by CSAMT some mineral indications may be expected.

(2) Summary of results

The hole is made up of andesitic volcanics and porphyry that have undergone hydrothermal alteration. The hydrothermal alteration can be divided into quartz-sericitized, siliceous argillized, and chloritized zones. The andesitic volcanics and porphyry belonging to the siliceous argillized and chloritized zones below 206 m are disseminated with pyrite. The pyrite dissemination is particularly conspicuous in the chloritized zone accompanying the potassium addition and albitization below 404.30 m, and is accompanied by chalcopyrite. There is a tendency for the copper grade to be high in the places mentioned above and around the border between the andesitic volcanics and the porphyry.

The position coordinates of the hole and drilling details are as given below:

Coordinates:	7,143,220.00N	399,180.00E	1,459.98m above sea level
Drilling details:	Direction N90°W	Inclination -35°	Depth 500.00m

2. Geology

(1) Litho Units

Depth	Original rock	Alteration Zone	Mineralization
0.00- 62.90m	andesitic autobrecciated lava	quartz-sericite	hematite dissemination
62.90-171.50m	fracture zone	siliceous argillized	jarosite,limonite,hematite prominent
171.50-206.00m	andesitic autobrecciated lava	siliceous argillized	hematite dissemination
206.00-270.00m	porphyry	siliceous argillized	pyrite dissemination
270.00-331.15m	andesitic autobrecciated lava	siliceous argillized	pyrite dissemination
331.15-467.50m	andesitic lava	propylite, potassium addition in parts	pyrite dissemination
467.50-500.00m	porphyry	propylite, potassium addition in parts	pyrite dissemination

(2) Alteration

The quartz-sericitized zone covers the ground surface to a depth of approximately 50m. Underlying this, a siliceous argillized zone of mainly kaolinite extends for a depth of 100m. Due to the influence of a N-S fracture zone running adjacent to the hole, the greater part of the siliceous argillized zone shows intense kaolinization with concentrations of jarosite, limonite and hematite. In the lower part of the siliceous argillized zone the kaolinization grows weaker as chloritization grows stronger and shifts gradually to a chloritized zone. Potassium addition and albitization accompany chloritization in depth-ranges of 448.15m-467.5m and 478.90m-493.50m.

(3) Mineralization

Pyrite dissemination and/or film occurs in the porphyry and andesitic volcanics of the siliceous argillized and chloritized zones below 206.0m. The pyrite dissemination is particularly marked below 404.30m, where the chloritization is strong and accompanies potassium addition; here chalcopyrite dissemination can be found at depths of 430.00m-448.15m and 467.5m-500m.

3. Results of Ore Analysis

Places where the grade of T.Cu was 500ppm or above are shown below as the range of mineralization.

There is a tendency for the copper grade to be higher near the borders of the andesitic volcanics and porphyry in the lower parts of the siliceous argillized and chloritized zones.

Depth m - m	Range m	T.Cu ppm	S.Cu ppm	Mo ppm	Au ppm	Ag ppm	T.Fe %	Original Rock	Alteration Zone
206 209	3	2167	<10	7	0.06	<0.4	3.01	Andesite/Porphyry	Siliceous argillized zone
238 239	1	1860	68	7	<0.04	<0.4	3.84	Porphyry	Siliceous argillized zone
316 317	1	506	38	20	<0.04	0.6	4.24	Andesite	Siliceous argillized zone
399 400	1	710	<10	10	<0.04	0.6	5.60	Andesite	Chloritized zone
430 433	3	675	26	11	<0.04	1.2	7.81	Andesite	Chloritized zone
437 438	1	666	16	14	<0.04	<0.4	5.68	Andesite	Chloritized zone
471 474	3	611	19	24	<0.04	<0.4	4.32	Porphyry	Chloritized zone
492 493	1	85	<10	20	4.80	<0.4	5.68	Porphyry	Chloritized zone

4. Comparison with CSAMT results

The intensely argillized fracture zone with concentrations of jarosite, limonite and hematite found at this hole at a depth of 62.90-171.50m corresponds to a low resistivity band of <100 ohm.m. Porphyry and andesitic volcanics with pyrite dissemination in the siliceous argillized and chloritized zones below 206.0m, correspond to a medium resistivity area of 100-300 ohm.m.

2-3-5 MJCV-5

1. Outline

(1) Reasons for boring

This hole is located on the southwestern hill side of the Sierra Overa (1,681m). From the fact that low-to-medium resistivity band of 0-300 ohm.m by CSAMT survey (ENAMI, 1993) is widely distributed, some mineral indications may be expected.

(2) Summary of results

The hole is made up of andesitic volcanics and porphyry that have undergone hydrothermal alteration. The hydrothermal alteration can be divided into intensely silicified, siliceous argillized and chloritized zones in descending order. The dioritic porphyry belonging to the chloritized zone below 363.9m is disseminated with pyrite, and minute traces of cuprite dissemination may be found under the microscope. There is a tendency for the copper grade to be higher in the porphyry and fracture zones.

The position coordinates of the hole and drilling details are as given below:

Coordinates: 7,142,000.00N 396,400.00E 1,550.98m above sea level

Drilling details: Direction N90°W Inclination -55° Depth 400.00m

2. Geology

(1) Litho-Units

Depth	Original rock	Alteration Zone	Mineralization
0.00-219.10m	andesitic lava	intensely silicified	hematite dissemination
219.10-321.40m	fracture zone	siliceous argillized	jarosite,limonite,hematite prominent
321.40-363.90m	porphyry	siliceous argillized	hematite dissemination
363.90-400.00m	dioritic porphyry	propylite	pyrite dissemination

(2) Alteration

The intensely silicified zone covers the mountainside to a depth of approximately 200m. The siliceous argillized zone underlying the silicified zone extends for a depth of 100-300m.

Due to the influence of a N-S fracture zone running adjacent to the hole, the greater part of the siliceous argillized zone shows intense kaolinization with concentrations of jarosite, limonite and hematite. The porphyry occurring below 321.4m shifts at 363.9 from siliceous argillized to chloritized zones.

(3) Mineralization

Pyrite dissemination is marked in the dioritic porphyry of the chloritized zone below 363.90m. Below 385.25m cuprite dissemination may be found associated with pyrite.

3. Results of Ore Analysis

Places where the grade of T.Cu was 500ppm or above are shown below as the range of mineralization.

There is a tendency for the copper grade to be higher in the fracture zone occurring in the border area between the dioritic porphyry and andesitic volcanics of the chloritized zone, and in the dioritic porphyry.

Depth m - m	Range m	T.Cu ppm	S.Cu ppm	Mo ppm	Au ppm	Ag ppm	T.Fe %	Original Rock	Alteration Zone
280 292	12	540	127	<5	<0.04	<0.4	6.24	(Fracture Zone)	Siliceous argillized zone
364 367	3	1041	469	6	<0.04	<0.4	5.44	Diolitic porphyry	Chloritized zone

4. Comparison with CSAMT results

The intensely silicified zone to a depth of 206.90m from the surface corresponds to a medium- to-high resistivity band of >100 ohm.m. Especially, from the fact that high resistivity band displays a configuration that hangs down deep in the lower part of the hole, it may be expected to develop toward the lower part of the silicified zone.

The range of the siliceous argillized zone corresponds to a low resistivity band of 0-100 ohm.m. Of this, the extremely low resistivity band of 0-16 ohm.m is thought to be due to the influence of the markedly kaolinized fracture zone with jarosite, limonite and hematite. The porphyry weakly disseminated with pyrite below 363.90 m is also within the 0-16 ohm.m range, but this is thought to be due to the influence of the alteration above it.

2-3-6 Consolidation of Survey Results

The rocks observed at each hole are andesitic volcanics of Cretaceous Aeropuerto formation, porphyry intruding into them, and altered rocks originating from these rocks. Below are given the characteristics of each type of rock.

1. Andesitic volcanics

These rocks are made up of porphyritic and/or aphanitic andesitic lava, autobrecciated lava, tuff and lapilli tuff, and form the basement of the region.

These rocks have undergone silicification, kaolinization, sericitization and chloritization and the initial minerals have altered; in many places the texture of the original rock is indistinct.

2. Porphyry

Porphyry occurs as small bodies comprised of andesite- or diorite-porphyry penetrating the andesitic volcanics; to the naked eye, porphyry displays sub volcanic texture like a tuff and/or autobrecciated lava, and there are places where the border with andesitic volcanics is indistinct. Porphyry has phenocryst of quartz and plagioclase, but these primary minerals have altered through undergoing silicification, kaolinite argillization, sericitization, chloritization and potassium addition.

3. Altered rocks

These rocks are originally the rocks described above that have undergone hydrothermal alteration; they form the mass of the Cerro Veraguas and the Sierra Overa. ENAMI (1987) has divided them into 4 groups; intensely silicified, quartz-sericitized, siliceous argillized and chloritized(propylitized) zones; based on the main altered minerals.

(1) Intensely-silicified, quartz-sericitized zones

These zones cover the ridge of the Cerro Veraguas and the Sierra Overa to a depth of 50-200m. The boundary between the two zones is indistinct. The zones are an aggregate of fine massive secondary quartz, filled by sericite and kaolinite between the crystals; film of alunite and natroalunite, and hematite dissemination and film, are also observed.

(2) Siliceous argillized zone

This zone occurs to a thickness of 100-300m beneath the intensely silicified and quartz-sericitized zones, and is also markedly developed along the fracture zone. It is made up mainly of quartz, kaolinite, sericite and pyrophylite, and films of alunite, natroalunite and gypsum are observed. Hematite dissemination and film may be observed throughout the zone, and along the fracture zone concentrations of hematite, limonite, jarosite and natrojarosite occur together with kaolinite clay.

Also, towards the lower part of this zone, the kaolinization becomes weaker and there is a gradual shift into the chloritized zone. Together with the appearance of the chlorite, pyrite dissemination and film may be observed.

(3) Chloritized zone

In this zone the primary mafic minerals of the original andesite and porphyry have undergone chloritization; the texture of the original rocks remains. Observation under the microscope shows that the quartz has undergone corrosion and the plagioclase has undergone sericitization and kaolinization. At MJCV-4, in addition to the development of films of gypsum and anhydrite, the potassium addition and albitization accompanying the chloritization dominate below 448.15m.

4. Mineralization

Hematite dissemination may be observed throughout the intensely silicified, quartz-sericitized and siliceous argillized zones with andesite volcanics as the original rock. In particular, there are strong concentrations of hematite, limonite and jarosite along the fracture zones developed along a N-S, NE-SW and NW-SE directions.

Pyrite dissemination and/or film dominates in the porphyry and andesitic volcanics in the lower part of the siliceous argillized zone and in the chloritized zone, and is accompanied by chalcopyrite, chalcocite, covelline, cuprite, sphalerite and galena.

Minerals observed at each hole are shown below.

Drill Hole	Cu Minerals	Other Ore Minerals
MJCV-1	chalcopyrite, chalcocite, covelline	
MJCV-2	chalcopyrite	sphalerite, galena
MJCV-3	chalcopyrite, chalcocite, covelline	
MJCV-4	chalcopyrite	
MJCV-5	chalcopyrite, covelline, cuprite	

The results of the ore analysis show a maximum copper grade of 7000ppm, and did not lead directly to the discovery of deposits, but copper mineralization was discovered in the following places:

1) The displacement area of the chloritized and siliceous-argillized zones within the porphyry. (MJCV-4)
2) The border area between the porphyry and the andesitic volcanics in the lower part of the siliceous-argillized and the chloritized zone. (MJCV-1,3,4)
3) Within the porphyry and the adjacent fracture zone. (MJCV-2,5)

Of these, overlapping the copper mineralization below 300m in the MJCV-3 hole (max. 7000ppm T.Cu, 368m-369m), molybdenum mineralization (average 52.4ppm Mo (300m-375m), max. 213ppm Mo) was discovered, indicating the special features of porphyry copper deposits. Furthermore below 490m in the MJCV-4 hole around the potassic zone, gold mineralization (0.6ppm-4.8ppm Au) was also discovered.

5. Comparison with CSAMT results

Comparison of the above geological, conditions with the CSAMT results (ENAMI, 1993) clarified the following correspondences.

1) High resistitivity band (>300 ohm.m)

Intensely silicified zone or new rocks. The deep hanging-down of the high resistitivity areas seen in and around the MJCV-3 and MJCV-5 holes is predicted to indicate the downwards development of the strongly-silicified zone.

Also, it is predicted that deep high resistitivity bands indicate the occurrence of a fresh or weakly-altered intrusive rocks.

2) Medium resistitivity band (100-300 ohm.m)

Pyrite-disseminated andesite and porphyry in the chloritized and the lower part of siliceous-argillized zones.

3) Low resistitivity band (<100 ohm.m)

Siliceous-argillized zone. In particular, fracture zones with marked argillization correspond to a range of 20 ohm.m and under.

2-4 Considerations

2-4-1 Geology and Mineralizing Alteration

Using the data from the 5-holes, 2,053m boring carried out in this phase, drilling geological profiles and synthetic columns were drawn up and a study was made of the geological structure, the spread of the mineralization effect and the connection between the two. The drilling geological profile for each hole is shown in Fig. II-2-1 (1)-(4), and the synthetic columns in Fig. II-2-2 (1)-(5).

1. Cerro Veraguas summit district (MJCV-1 & MJCV-2)

The district is made up of andesitic volcanics and porphyry that have undergone hydrothermal alteration, and the conjugate fracture zones with a NE-SW and NW-SE direction are developed. From the fact that porphyry made continuous appearances at a height above sea level of about 1,650m in both MJCV-1 and MJCV-2, it is supposed that it intruded controlled by the fracture zone with a NE-SW direction close to the east-west section.

Hydrothermal alteration is zonalized, from the top down, into intensely silicified/quartz-sericitized transition zone, siliceous-argillized zone and chloritized zone. In the lower part of the siliceous-argillized zone and in the chloritized zone, quartz, sericite and pyrite are found universally, as well as kaolinite and chlorite, corresponding to the phillic zone of the hydrothermal alteration classification of porphyry copper deposits according to Lowell and Guilbert (1970). Each zone possesses a brecciated or pseudobrecciated structure, the matrix has undergone kaolinization and sericitization, and hematite, limonite and jarosite are developed in stockwork form; from which it may be considered that brecciation occurred at the time of hydrothermal activity.

Copper mineralization is found in the border area between the porphyry and andesitic volcanics in the lower part of the siliceous-argillized and the chloritized zone and along the fracture zone within the porphyry, but since the copper grade at T.Cu 500-1100ppm is low, and is accompanied as shown in the MJCV-2 hole by the mineralization effect of small amounts of lead and zinc, it is supposed that the region is some distance from the center of the mineralization.

2. Cerro Veraguas southern district (MJCV-3)

The district is made up of andesitic volcanics and porphyry that have undergone hydrothermal alteration, and the conjugate fracture zones with a NE-SW and NW-SE direction are developed. From the fact that porphyry cuts the andesitic volcanics like a dike in shape at depths below 1,600 m above sea level, it is assumed that it split from the surrounding stock-form porphyry.

Like the Cerro Veraguas summit district, hydrothermal alteration is zonalized, from the top down, into intensely silicified/quartz-sericitized transition zone, siliceous-argillized zone and chloritized zone. In the lower part of the siliceous-argillized zone and in the chloritized zone, quartz, sericite and pyrite are found universally, as well as kaolinite and chlorite, corresponding to the phillic zone of the hydrothermal alteration classification of porphyry copper deposits according to Lowell and Guilbert (1970). Each zone possesses a brecciated or pseudobrecciated structure, the matrix has undergone kaolinization and sericitization, and hematite, limonite and jarosite are developed in stockwork form, from which it may be considered that brecciation occurred at the time of hydrothermal activity.

Also, from the CSAMT results, on both the east and west sides of the MJCV-3 hole the fact that the high resistitivity band corresponding to the intensely-silicified zone displays a form that hangs down deep suggests that the intensely silicified zone has developed downwards as a result of its being at the center of the hydrothermal alteration.

Copper mineralization was discovered in the porphyry of the chlorite zone below 300m of the MJCV-3 hole, in particular in the border area with the andesitic volcanics, and at 10 points, a total of 14m, had a 500-7000ppm T.Cu.

In these spots there is also an overlapping with molybdenum mineralization, an average of 52.4ppm Mo between 300m-375m, with a maximum of 213ppm Mo, indicating the special features of porphyry copper deposits. Thus the existence of porphyry copper deposits in this area may be expected, and there is a need for prospecting to continue.

3. Sierra Overa eastern district (MJCV-4)

The district is made up of andesitic volcanics and porphyry that have undergone hydrothermal alteration, and a fracture zone is developed in a N-S direction. From the fact that porphyry cuts the andesitic volcanics like a dike in shape at altitudes below 1,350 m above sea level, it is assumed that it split from the surrounding stock-form porphyry.

The hydrothermal alteration is zonalized, from the top down, into a quartz-sericitized zone, a siliceous-argillized zone and a chloritized zone. The lower part of the siliceous-argillized zone and the chlorite zone, below 206m of the MJCV-4 hole, are made up of quartz, sericite, gypsum, anhydrite and pyrite, as well as kaolinite and chlorite, and the chloritized zone, between 448.15m-467.5m and between 478.9m-493.5m, is rich in albite and potassium feldspar. Thus the former corresponds to the phillic, and the latter to the potassic, zone of the hydrothermal alteration classification of porphyry copper deposits according to Lowell and Guilbert (1970).

These zones of alteration possess an brecciated or pseudobrecciated structure, the matrix has undergone silicification, kaolinization and sericitization, and hematite, jarosite and limonite are developed in stockwork form, from which it may be considered that brecciation occurred at the time of hydrothermal activity.

In addition, the fracture zone between 62.9m-171.5m shows marked kaolinization, with concentrations of hematite, jarosite and limonite; from this it is possible that the fracture zone in a N-S direction may have been a passage for hydrothermal solution.

Copper mineralization was found in/around the border area between the porphyry and andesitic volcanics in the lower part of the siliceous-argillized zone and in the chloritized zone and around the potassic zone mentioned above below 206m of the MJCV-4 hole, and 7 points a total of 13m had a 500-3200ppm T.Cu. Around the potassic zone below 490m, a gold mineralization (0.6-4.8ppm Au) was also discovered.

From the existence of geochemical anomalies in copper and molybdenum in and around the area, and the existence of the San Juan mine some 1,500m to the NW from the hole MJCV-4, the existence of porphyry copper deposits in this area may be expected, and there is a need for prospecting to continue.

4. Sierra Overa southwest district (MJCV-5)

The district is made up of andesitic volcanics and porphyry that have undergone hydrothermal alteration, and a fracture zone is developed in a N-S direction. From the fact that the porphyry is continuous below 1,300m above sea level, the existence of stock-form porphyry may be presumed.

From the fact that a intensely silicified zone continues from the ground surface to 206.9m of the hole MJCV-5 and corresponds to a CSAMT high resistitivity zone, it may be forecast to display a formation that hangs down deep. The siliceous-argillized zone and the chloritized zone below 206.9m are made up of quartz, sericite, gypsum, anhydrite and pyrite as well as kaolinite and chlorite, corresponding to the phillic zone of the hydrothermal alteration classification of porphyry copper deposits according to Lowell and Guilbert (1970).

These zones of alteration are massive and compact, with few places displaying an brecciated structure; but the fracture zone between 219.1m-321.4m shows marked kaolinization with concentrations of hematite, jarosite and limonite; from which it is possible that the fracture zone in a N-S direction may have been a passage for hydrothermal solution.

Copper mineralization was discovered between 280m-292m, where the porphyry and N-S fracture zone intersect, an average of 540ppm T.Cu, and between 364m-367m, the border area of the chlorite and siliceous clay bands within the porphyry, an average of 1,041ppm T.Cu; from this it is surmised that the copper mineralization was controlled by changes in the alteration environment within the porphyry, and by the N-S fracture zone of a passage for hydrothermal solution.

2-4-2 Homogenization temperature measurement of fluid inclusion

With regard to 14 samples of white mineral veins in the drilling core samples, double-side-polished thin sections were made, and homogenization temperature measurements of fluid inclusions were carried out; the measurements were taken in 9 samples except for those 5 samples in which no fluid inclusions were found.

For the homogenization temperature measuring a Metler FP5 (Control Unit) and FP52 (Hot Stage) were used for the temperature controller and heating stage, respectively. The temperature at which bubbles disappeared was measured to an accuracy of 1°C.

Minerals, used for the measuring, were quartz in 8 samples, calcite in one sample and anhydrite in one sample, and all the fluid inclusions were made up of both a liquid and a gas phase.

These inclusions are of primary origin and of 2-25 micro meter in size, and many of them showing an irregular granule form. The experimental results of the 121 inclusions measured are given in Table II-2-8. Fig. II-2-4 shows the distribution of the fluid inclusion homogenization temperatures.

The homogenization temperatures are distributed in the range 128°C-364°C. From the fact that homogenization temperatures of 300°C and over are all quartz or anhydrite veins in places accompanying copper mineralization within a chloritized zone, there may be considered to be a connection with the formation temperature of primary copper minerals such as chalcopyrite. Even in the same chloritized zone, most of the quartz and calcite veins in places accompanying potassium addition show a homogenization temperature of less than 200°C, thought to be the influence of hydrothermal solution on the primary mineralization.

Also, the homogenization temperature of quartz in intensely silicified zone was 176°C-297°C, and this is thought to indicate the crystallization temperature of secondary quartz due to silicification.

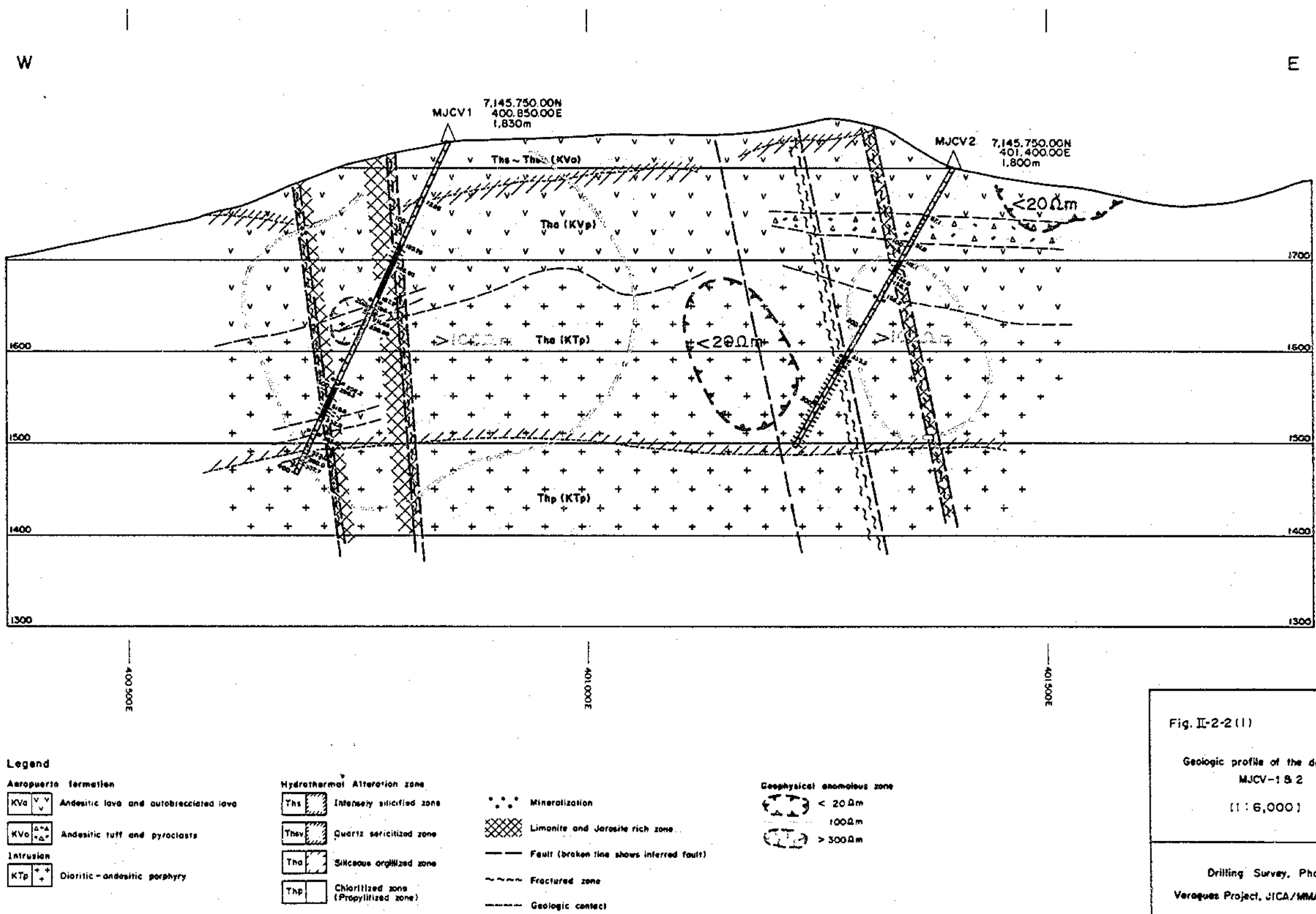

Fig. II-2-2 (1)

Geologic profile of the drill hole MJCV-1 & 2

(1 : 6,000)

Drilling Survey, Phase I

Veraguas Project, JICA/MMAJ-ENAMI

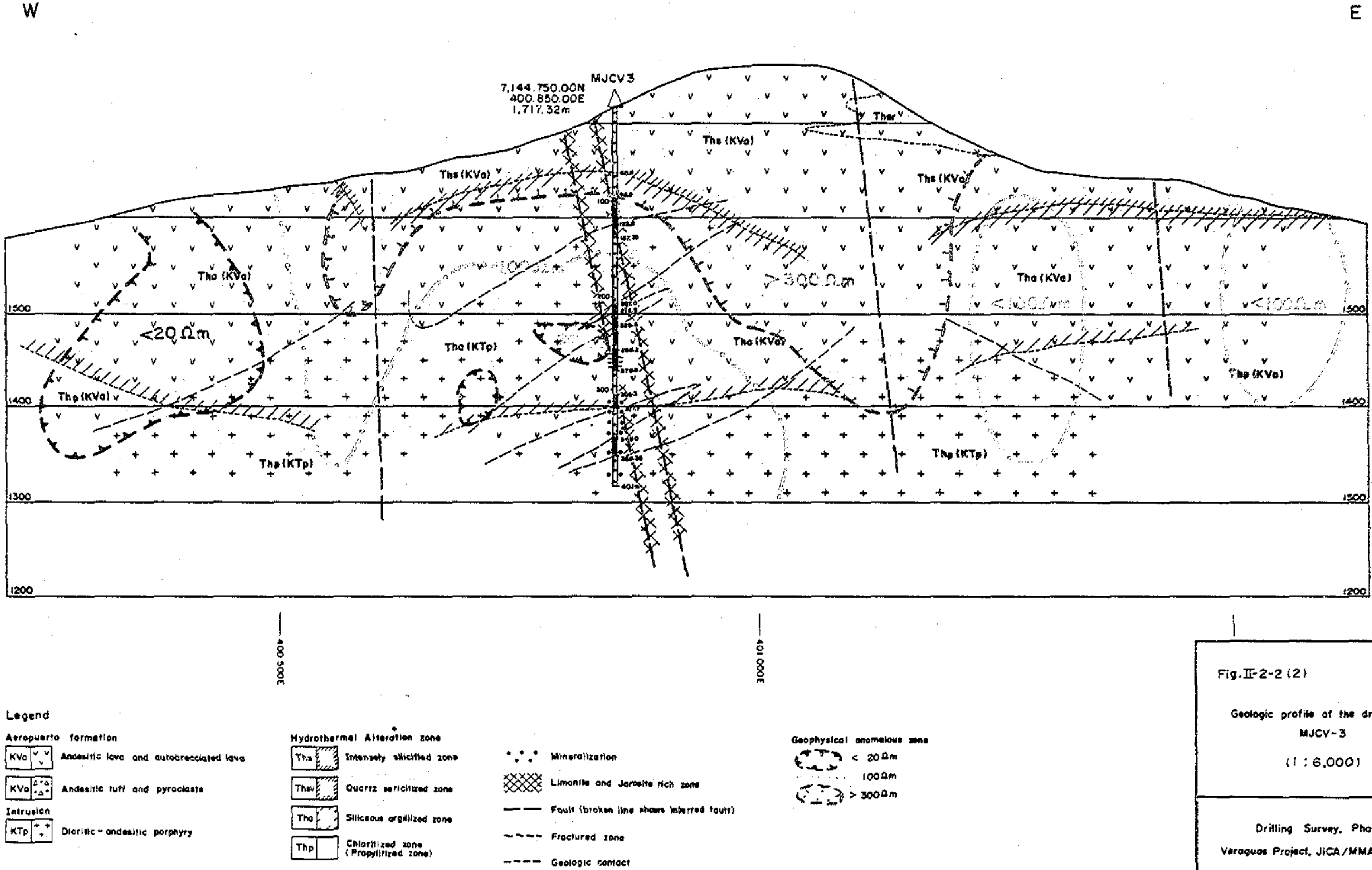

Fig.II-2-2 (2)

Geologic profile of the drill hole MJCV-3

(1 : 6,000)

Drilling Survey, Phase I

Veraguas Project, JICA/MMAJ-ENAMI

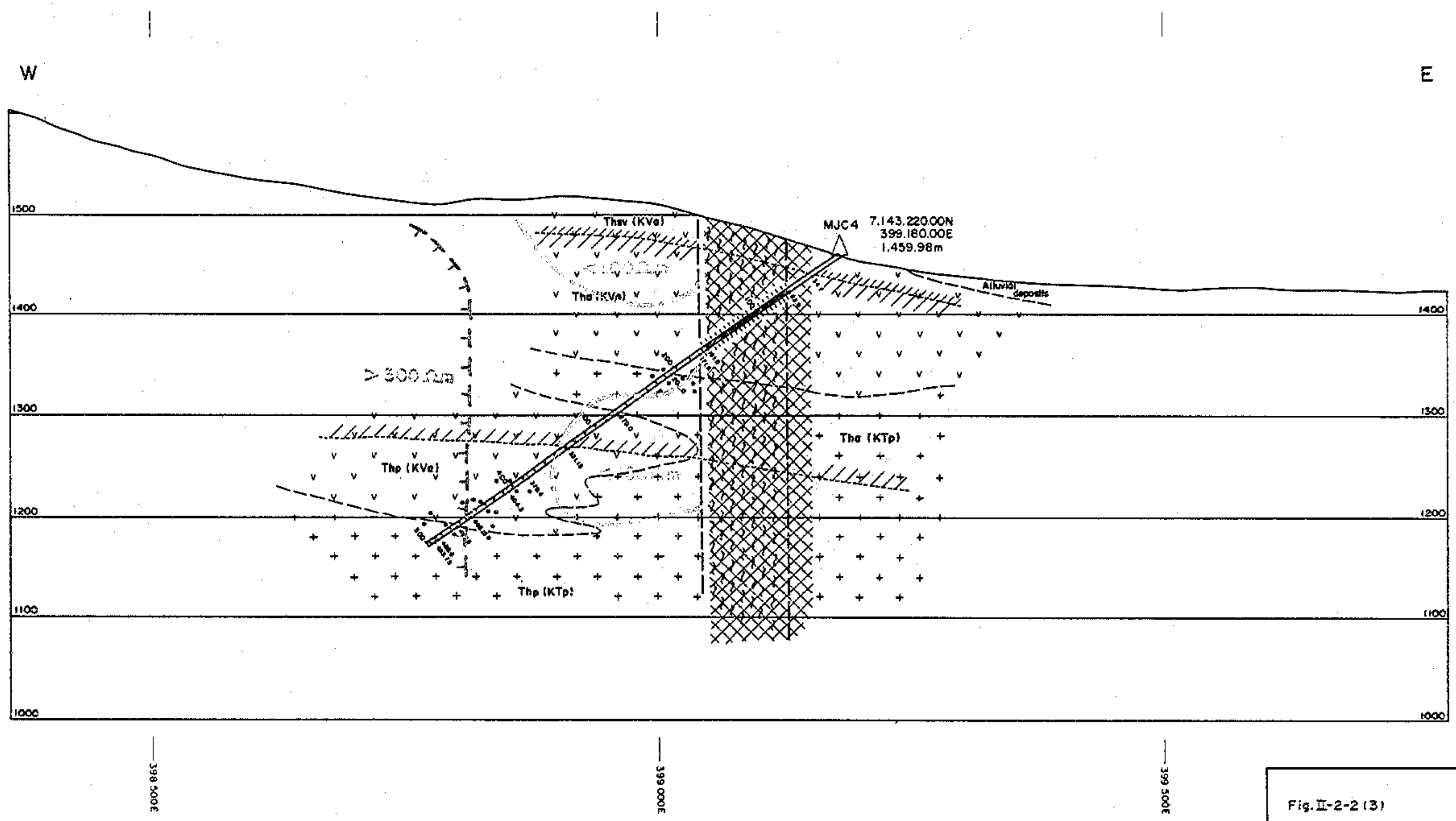

Legend

Aeropuerto formation

KVa — Andesitic lava and autobrecciated lava

KVa — Andesitic tuff and pyroclasts

Intrusion

KTp — Dioritic-andesitic porphyry

Hydrothermal Alteration zone

Ths — Intensely silicified zone

Thsv — Quartz sericitized zone

Tha — Siliceous argillized zone

Thp — Chloritized zone (Propylitized zone)

Mineralization

Limonite and Jarosite rich zone

Fault (broken line shows inferred fault)

Fractured zone

Geologic contact

Geophysical anomalous zone

< 20Ωm

100Ωm

> 300Ωm

Fig. II-2-2 (3)

Geologic profile of the drill hole MJCV-4

(1 : 6,000)

Drilling Survey, Phase I

Veraguas Project, JICA/MMAJ-ENAMI

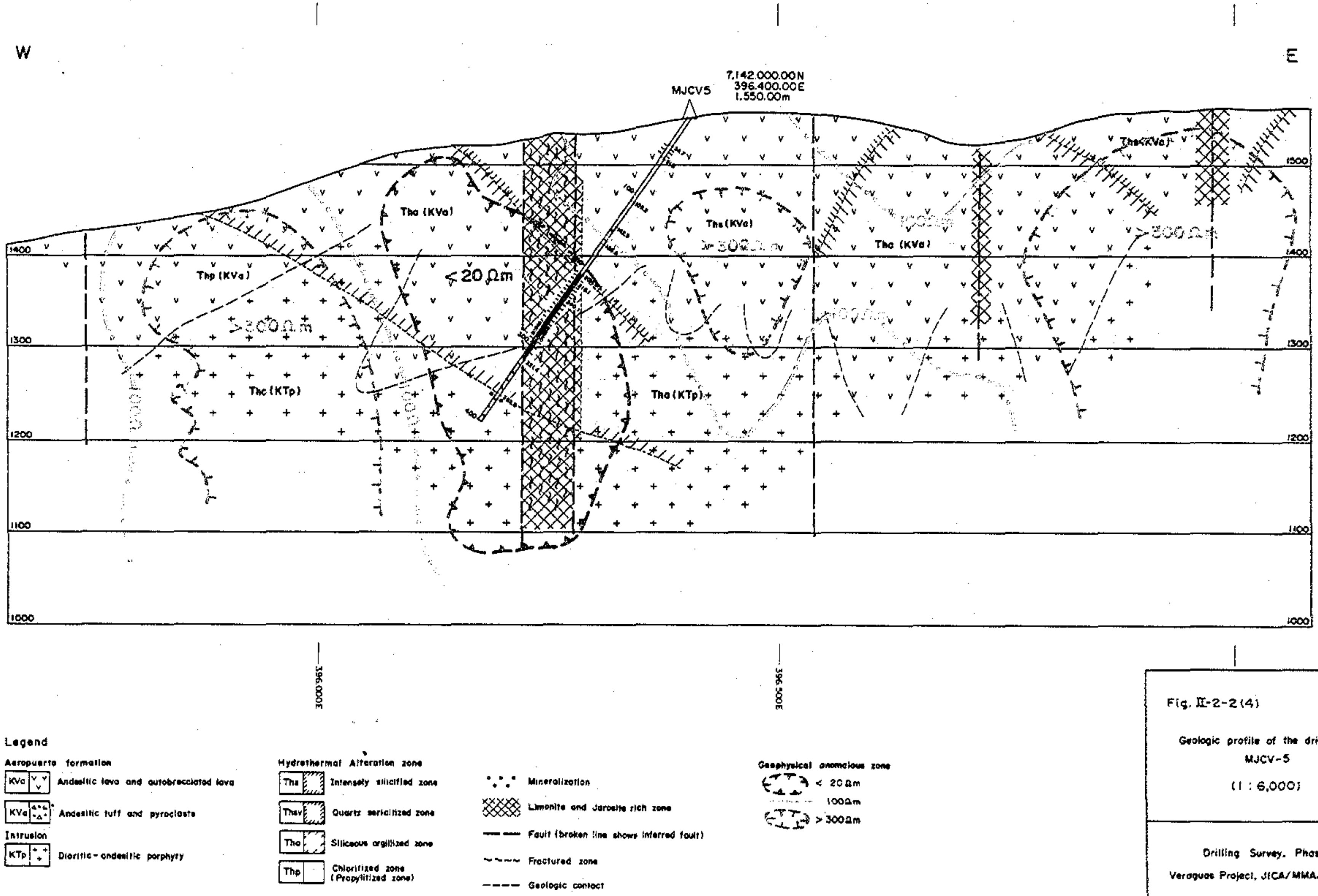

Fig. II-2-2(4)

Geologic profile of the drill hole MJCV-5

(1 : 6,000)

Drilling Survey, Phase I

Veraguas Project, JICA/MMAJ-ENAMI

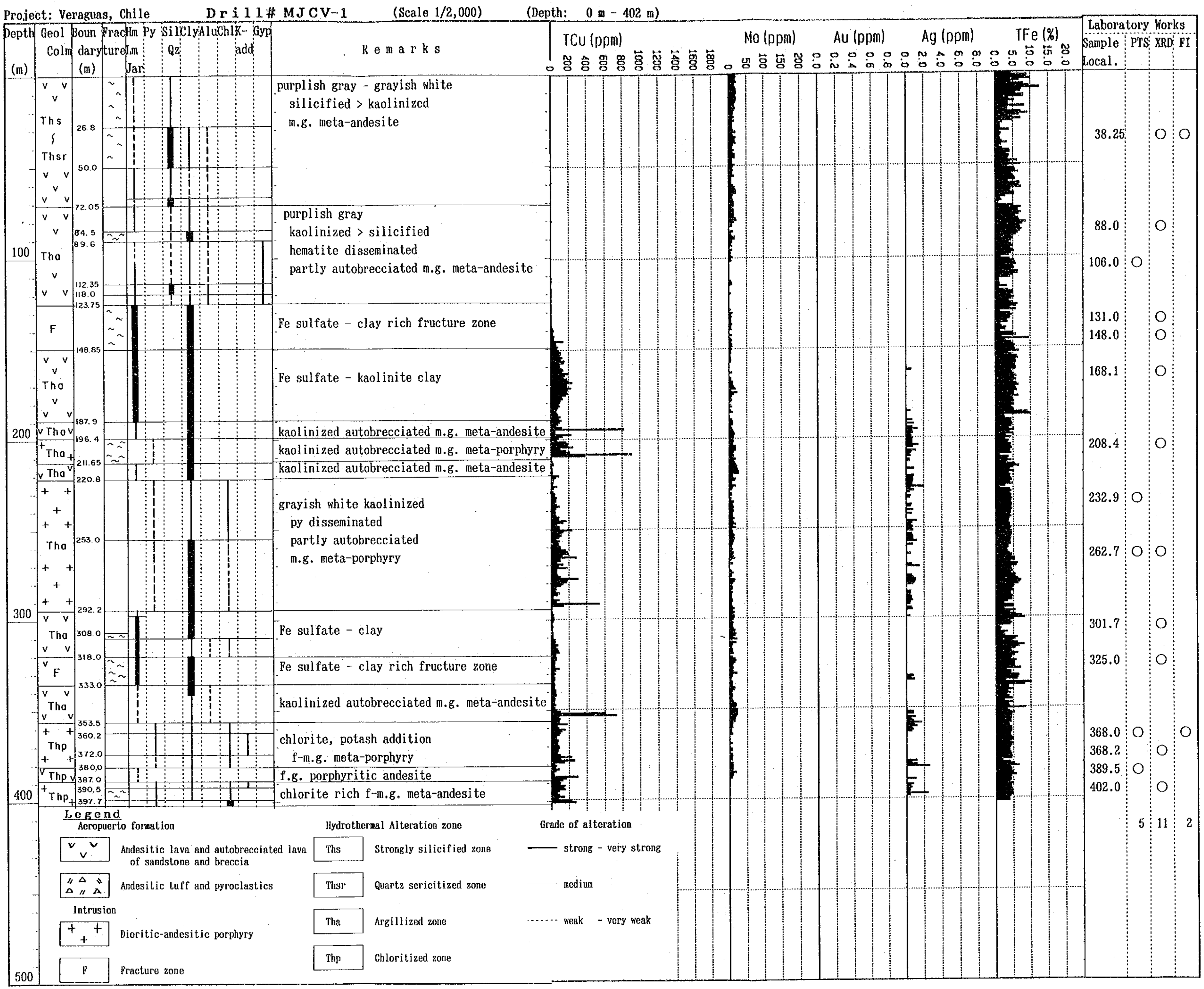

Fig.II-2-3(1) Synthetic column for MJCV-1 (1:2,000)

Project: Veraguas, Chile Drill# MJCV-2 (Scale 1/2,000) (Depth: 0 m - 350 m)

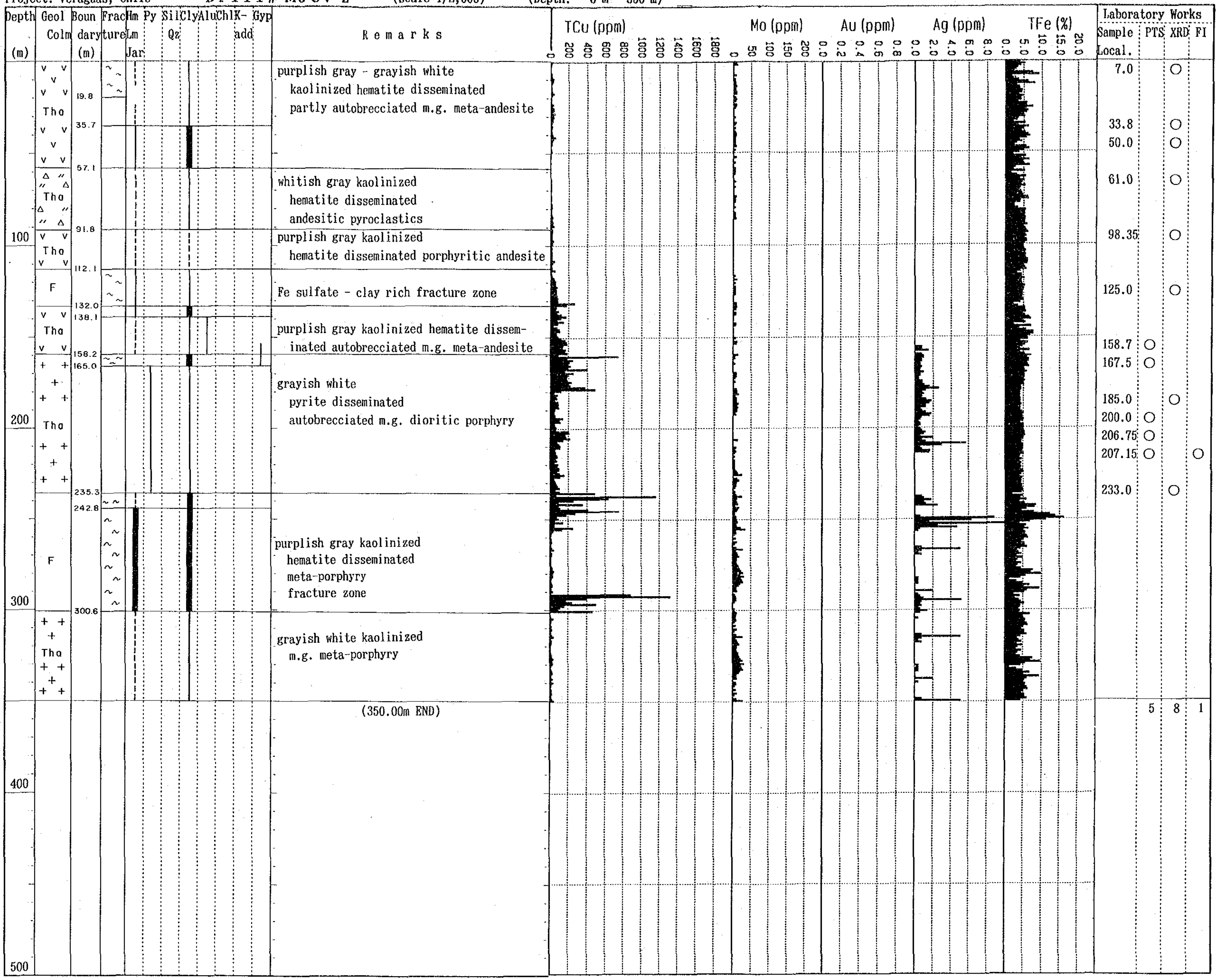

Fig.II-2-3(2) Synthetic column for MJCV-2 (1:2,000)

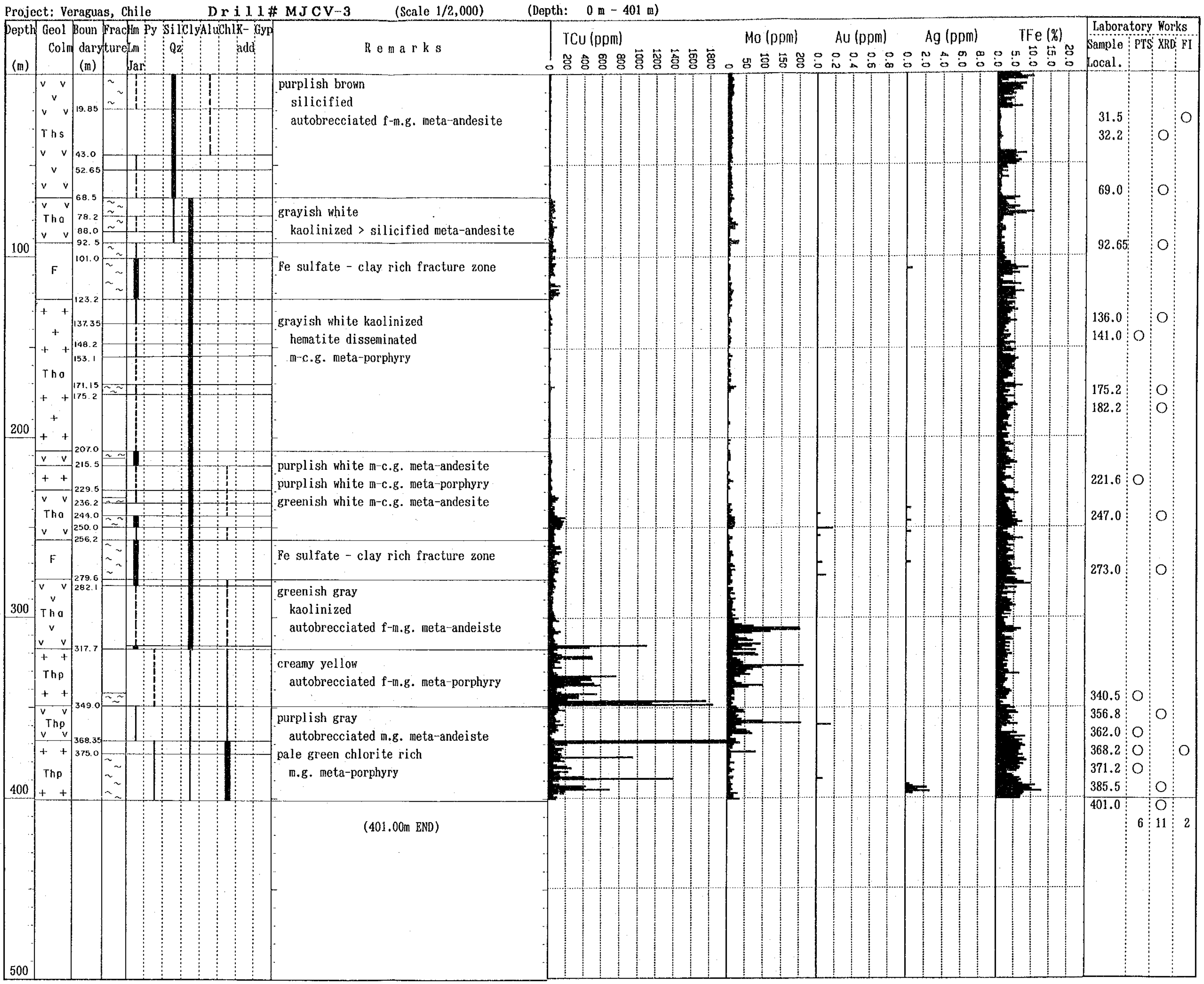

Fig.II-2-3(3) Synthetic column for MJCV-3 (1:2,000)

Project: Veraguas, Chile Drill# MJCV-4 (Scale 1/2,000) (Depth: 0 m - 500 m)

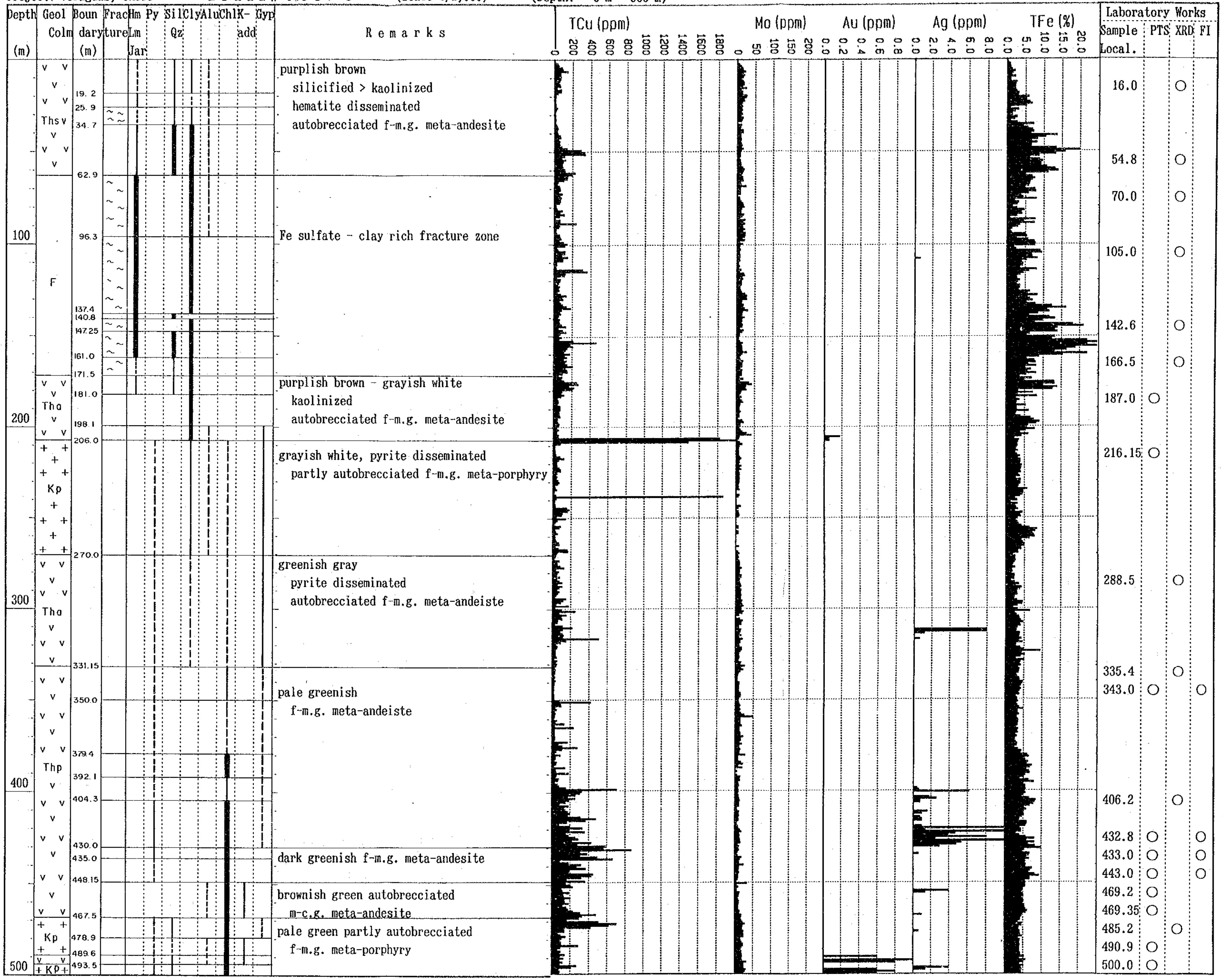

Fig.II-2-3(4) Synthetic column for MJCV-4 (1:2,000)

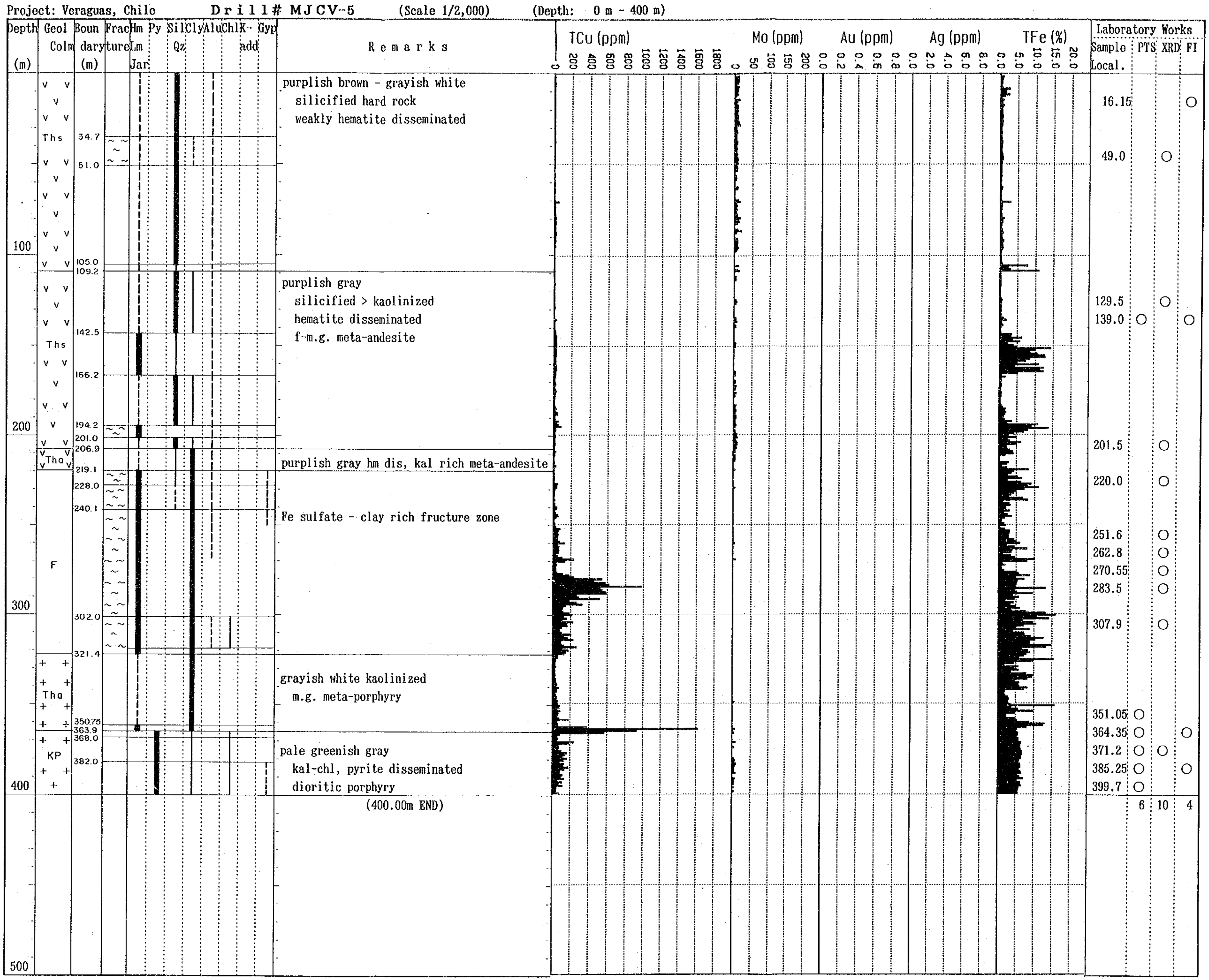

Fig.II-2-3(5) Synthetic column for MJCV-5 (1:2,000)

TableII-2-6 Results of the microscopic observation (Polished thin section)

Sample					Phenocryst			Original Texture of igneous rock	Alterlation Mineral										Ore Mineral													Remarks
No	Drill Hole	Depth (m)	Original Rock	Alt. Zone	Qz	Pl	Remarks		dgree of alteration	Qz	Ab	Bt	Se	Ch	Ka	Ah	Gp	Ca	Py	Po	Mc	Cp	Cv	Cc	Cu	Gn	Sp	Mt	Hm	Lm	Ge	
1	MJCV-1	106.00	Kva	Tha					strong	◎			○		△	○	·		·			·								·	·	
2	1	232.90	Kp	Tha	○		corrosion Qz	porphyritic		◎	○		△		○	·			◎			△										
3	1	262.70	Kp	Tha	△	◎	corrosion Qz	porphyritic		○			○						◎			○	·	○								
4	1	368.00	Kp	Thp					strong	◎			○		◎	·			◎	·		·	·	·			·					Cu minerals included in Py
5	1	389.50	Kp	Thp					strong	◎			○		○				◎			△	·	·								
6	MJCV-2	158.70	Kp	Tha					strong	○			○		◎				◎	·			·				·					
7	2	167.50	Kp	Tha		◎		porphyritic		◎	○		○		○			◎	◎			·				△	△					later stage veinlet of Pb & Zn
8	2	200.00	Kp	Tha	○	△	corrosion Qz	porphyritic		◎	△		◎		○				◎													
9	2	206.75	Kp	Tha	○	◎	corrosion Qz	porphyritic		○	○		△		○				◎							△	◎					later stage veinlet of Pb & Zn
10	2	207.15	Kp	Tha	△	◎	corrosion Qz	porphyritic		○	○		△		○				◎							○	○					later stage veinlet of Pb & Zn
11	MJCV-3	141.00	Kp	Tha	○		corrosion Qz	porphyritic		◎		·	○	·	△				·										·	·	·	
12	3	221.60	Kp	Tha	○		corrosion Qz	porphyritic		◎			△		○				·										·	·	·	
13	3	340.50	Kp	Thp		◎		porphyritic		○			△	·	○				◎			·	·									
14	3	362.00	Kva	Thp	△			porphyritic		◎			○	·	○	·			·											·	·	
15	3	368.20	Kva	Thp					strong	◎			△		◎				◎			·		·								
16	3	371.20	Kp	Thp					strong	◎			○		◎	·			◎		○	·	△				·					
17	MJCV-4	187.00	Kva	Tha	△		corrosion Qz		strong	◎	·		△		○		△		·											·	·	
18	4	216.15	Kp	Tha					strong	○			○		◎		◎		◎								·					
19	4	343.00	Kva	Thp					strong	◎	△		◎		○				◎			·					·					high Cu content
20	4	432.80	Kva	Thp					strong	△			·	○		◎	·	◎	◎			○					·					high Cu content
21	4	433.00	Kva	Thp		○			strong	○	○		·	△	○	◎		◎	◎	·		○							△			high Cu content
22	4	443.00	Kva	Thp					strong	△	△		△	·	△	◎	△	◎	◎			○										high Cu content
23	4	469.20	Kp	Thp	○	◎		porphyritic		◎	◎		○	△		△	○	○	◎			◎					·	·				high Cu content
24	4	490.90	Kva	Thp	△	◎		porphyritic		◎	◎		○		△	◎	△		◎	·		△						·				high Cu content
25	4	500.00	Kvp	Thp	△	◎		porphyritic		◎	◎		○		△	○			◎	·		△						·				high Cu content
26	MJCV-5	139.00	Kva	Ths					strong	○			△		○																	
27	5	351.05	Kp	Tha					strong	○					◎															·		
28	5	364.35	Kp	Thp					strong	○			·		◎				◎	·												
29	5	371.20	Kp	Thp					strong	○	△		·	·	○				◎													
30	5	385.25	Kp	Thp		◎		porphyritic		○			○	△					◎	·		·			○							
31	5	399.70	Kp	Thp		◎		porphyritic		△			·			·		○	◎			·	·		△							

[abandance]
◎:abandant
○:common
△:minor
·:rare

[Mineral names]
Qz:quartz
Pl:plagioclase

[Mineral names]
Qz:quartz
Ab:albite
Bt:biotite
Se:sericite
Ch:chlorite
Ka:kaolinite
Ah:anhydrite
Gp:gypsum
Ca:carbonate

[Mineral names]
Py:pyrite
Po:pyrrhotite
Mc:marcasite
Cp:chalcopyrite
Cv:covellinite
Cc:chalcocite
Cu:cuprite
Gn:garena
Sp:sphererite
Mt:magnetite
Hm:hematite
Lm:limonite
Ge:goesite

Table II-2-7 Results of the powder X-ray diffraction

Classification		Abbr.	Mineral Name	Chemical Formula	Drill Hole Depth (m)	1 MJCV-1 38.25m	2 MJCV-1 88.00m	3 MJCV-1 131.00m	4 MJCV-1 148.00m	5 MJCV-1 186.10m	6 MJCV-1 208.40m	7 MJCV-1 262.70m	8 MJCV-1 301.70m	9 MJCV-1 325.00m	10 MJCV-1 368.00m	11 MJCV-1 402.00m	12 MJCV-2 7.00m	13 MJCV-2 33.80m	14 MJCV-2 50.00m	15 MJCV-2 61.00m	16 MJCV-2 98.35m	17 MJCV-2 125.80m	18 MJCV-2 185.00m	19 MJCV-2 233.00m	20 MJCV-3 32.20m	21 MJCV-3 69.00m	22 MJCV-3 92.65m	23 MJCV-3 136.00m	24 MJCV-3 175.20m	25 MJCV-3 182.20m	26 MJCV-3 247.00m	27 MJCV-3 273.00m	28 MJCV-3 356.80m	29 MJCV-3 385.50m	30 MJCV-3 401.00m	31 MJCV-4 16.00m	32 MJCV-4 54.80m	33 MJCV-4 70.00m	34 MJCV-4 105.00m	35 MJCV-4 142.60m	36 MJCV-4 166.50m	37 MJCV-4 288.50m	38 MJCV-4 335.40m	39 MJCV-4 406.20m	40 MJCV-4 485.20m	41 MJCV-5 49.00m	42 MJCV-5 129.50m	43 MJCV-5 201.50m	44 MJCV-5 220.00m	45 MJCV-5 251.60m	46 MJCV-5 262.80m	47 MJCV-5 270.55m	48 MJCV-5 283.50m	49 MJCV-5 307.90m	50 MJCV-5 371.20m
Silicate	Silica	Qz	Quartz	SiO2		◎	◎	◎	◎	◎	◎	◎	◎	◎	◎	◎	△	◎	◎	◎	◎	◎	◎	◎	◎	◎	◎	◎	◎	◎	◎	◎	◎	△	◎	◎	◎	◎	◎	◎	◎	·	◎	◎	◎	◎	◎	◎	◎	◎	◎	◎	◎	◎	◎
	Clay	Chm	Chamosite	(Fe,Al,Mg)6(Si,Al)4O10(OH)8																														·															△			·			
		Chl	Chlorite	(Mg,Fe,Al)12(Fe,Al,Si)8O20(OH)16												○							·	○											△					·				·	△		△						○		
		Dck	Dickite	Al2Si2O5(OH)4											△												△							○		·	○	○		△														○	
		Kal	Kaolinite	Al2Si2O5(OH)4		○	◎	△	◎	·	△	△			○		◎	◎	◎	△		△				△	◎	◎	○					◎	○				△	△		·											△		△
		Nac	Nacrite	Al2Si2O5(OH)4											△						○													○	○											△	△								
		Hal	Halloysite	Al2Si2O5(OH)4·2H2O		△																																					·							·					
		Pyrf	Pyrophyllite	AlSi4O10(OH)2		△	◎	△			△		△	○	△		◎	◎	◎	○		△	△	·																															
		Mus	Muscovite	K·Al2(Si3Al)O10(OH,F)2		△		△	○		△	△	△		○	△				△		◎	○	△			△		○		△		△	◎	◎	△			△		◎				△	△	△	△	△	△	△	△	○	△	△
		Tlc	Talc	Mg2Si4O10(OH)2																																											·		△						
		Prg	Paragonite	NaAl2(AlSi3O10)(OH)2										△																																									
	Cu	Sht	Shattuckita	Cu5(SiO3)4(OH)2					·	·	·								·			·																·																	
	Other	Olg	Oligoclase	(Na,Ca)(Al,Si)4O8												◎							·																						○									·	
		Ab	Albite	(Na,Ca)(Al,Si)4O8						○	○	◎				◎							△	·																				◎	○								△		·
		Or	Orthoclase	(K,Na)(Al,Si)4O8			△		○	·		△	○	△		·		△	△		·							·	·	○		△					·	·			○														
		Mic	Microcline	KAlSi3O8		△		△			△				△							△	·	△							·			·	·										△	△		△		△	△	△	△	△	△
		Di	Diposide	CaMg(SiO3)2																					△				◎		△																								
		Trm	Tremolite	Ca2(Mg)5Si8O22(OH)2																			△											△																					
		Act	Actinolite	Ca2(Mg,Fe)5Si8O22(OH)2				△																			△	·	·		△		△	△			·	·	△	·															
		Rie	Riebeckite	(Na,Ca)2(Mg,Fe)5Si8O22(OH)2			·																													△																			·
		Bt	Biotite	K(Mg,Fe)2AlSi3O10(OH)2								△		△																								·																	
		Tur	Tourmaline	(Na,Ca)Al3(Al,Fe,Mn)6(OH,F)4(BO3)3(SiO3)6				·						·		·																																		○				△	·
		Zny	Zunyite	Al13Si5O20(OH,F)18Cl															△	△						○											△	·													△	△			
Sulfate	Fe	Jar	Jarosite	(K)Fe3(SO4)2(OH)6									△										·						·																										
		Na-Jar	Natrojarosite	(K,Na)Fe3(SO4)2(OH)6							·						△						·																		△			△											
		Btl	Butlerite	Fe(SO4)(OH)·2H2O																																					·														
		Prb	Parabutlerite	Fe(SO4)(OH)·2H2O									·																																										·
		Crl	Kornelite	Fe(SO4)3·7H2O					△																																														
		Rzn	Rozenite	Fe(SO4)·4H2O																				·																															
		Sdr	Siderotil	Fe(SO4)·5H2O									△																																										
	Cu	Cln	Chalcanthite	Cu(SO4)·5H2O										·							·			·			·				·													·											
		Ant	Antrelite	Cu3(SO4)(OH)4																			·																											·					
		Brc	Brochanthite	Cu4(SO4)(OH)6				·									·	·				·											·												·			·	·		·	·	·		
	Other	Alu	Alunite	(K)Al3(SO4)2(OH)6			○											○	○	△					○				·							○	△																	○	
		Na-Alu	Natroalunite	(K,Na)Al3(SO4)2(OH)6		◎								△	○		△								○						○		△			○	△	·								○	○	○	○	○	○				
		Kdm	Kademite	Al(SO4)(OH)4·5H2O																						·		·																								·			
		Alg	Alunogen	Al2(SO4)3·18H2O				·			△		△					△				○	△	△									·										△										△		
		Anh	Anhydrite	Ca(SO4)																																							○	·											
		Gyp	Gypsum	Ca(SO4)·2H2O							△							·					△					△		○				·	·							·	·	△					·	△					
Sulphide	Fe	Po	Pyrrhotite	Fe7S8													·									△																													
		Apy	Arsenopyrite	FeAsS						·		·	·																																							·			
		Py	Pyrite	FeS2					△		△	○			○	△		·	△	△	·		○	○											△								△	·	△										○
	Cu	Tet	Tetrahedrite	Cu12Sb4S13																									·																										
		Ccs	Chalcosine	Cu2S																													·					·																	
		Djr	Djurleite	Cu31S16							·		·	·	·								·	·																				·	·		·						·		
		Ena	Enargite	Cu3AsS4						·		·																			·													·											·
		Cov	Coveline	CuS		·																																								·		·							
Oxide & Hydro oxide	Fe	Hm/Ht	Hematite	Fe2O3			△	○							△	△	◎	△	△	○	△	○	○				△	△	·	△	◎	△	△		△		△	○	○	△	△						·	○	○		○	○		△	
		Mgh	Maghemite	Fe2O3																						·							·												·		△			△	△		·	
		Mt	Magnetite	Fe3O4																											·	△						·		·															
		Akg	Akaganeite	FeO(OH)																																			·																
		Frx	Feroxyhyite	FeO(OH)													·											·			·		△					·			·											·			
		Goe	Goethite	FeO(OH)																											△										·							·			·	○			·
	Other	Akd	Akdalaite	(Al2O3)4·H2O																												△																							
		Bay	Bayerite	Al(OH)3													·									·				·		·																							
		Dsp	Dispore	AlO(OH)		△						△					·				△					·				·		○									·		·	-							○			△	
		Crp	Cryptomelane	K·Mn8O16						·																																													
		Gro	Groutite	MnO(OH)																																			·																
Other	Fe	Scr	Scorodite	Fe(AsO4)·2H2O					·				·																										·		·			△											
		Fml	Ferrimolybdit	Fe2(MoO4)3·nH2O					·																																														
		Pbk	Pseudobrookite	Fe2(TiO3)O2																																		·																	
		Prt	Pseudorutile	Fe2(TiO3)O9																																			·	·															
	Cu	Crb	Cornubite	Cu(AsO4)2(OH)4																	·																																		
		Atc	Atacamite	Cu2Cl(OH)3																								·																											
		Chn	Chnevixite	Cu2Fe2(AsO4)2(OH)2·H2O												·			·	·				·																															·
		Clc	Clinoclase	Cu3(AsO4)(OH)3																·																																			
	Other	Szf	Sulphur	S																																						·													
		Rut	Rutile	TiO2																																			△																

TableII-2-8 Homogenization temperature measurement of fluid inclusion

Drill Hole	Depth (m)	Original rock	Alteration zone	T.Cu ppm	Mineral	grain size(μ) Min. Max.	Numbers of inclusions	Min. (C°)	Max. (C°)	Ave. (C°)	S.D. (C°)
MJCV-1	38.25	Kva	Ths	5	no inclusion		0				
MJCV-1	368.20	Kp	Thp	73	quartz	5×2～20×10	8	209	290	253.9	31.7
MJCV-2	207.15	Kp	Tha	80	quartz	3×3～20×10	20	209	286	223.4	23.1
MJCV-3	31.50	Kva	Ths	16	quartz	5×3～25×10	20	176	297	236.4	39.0
MJCV-3	368.20	Kva	Thp	7,000	quartz	5×2	1		277		
MJCV-4	343.00	Kva	Thp	26	no inclusion		0				
MJCV-4	432.80	Kva	Thp	868	quartz anhydrite	6×3～20×10 10×3～20×12	11 9	268 207	334 241	312.2 228.0	19.9 15.2
MJCV-4	433.00	Kva	Thp	868	quartz	6×4～25×10	20	128	320	237.4	78.9
MJCV-4	443.00	Kva	Thp	366	calcite	8×4～20×10	20	150	189	161.4	11.6
MJCV-4	469.35	Kp	Thp	294	quartz	5×3～20×10	20	149	258	190.5	41.1
MJCV-5	16.15	Kva	Ths	14	no inclusion		0				
MJCV-5	139.00	Kva	Ths	14	no inclusion		0				
MJCV-5	364.35	Kp	Thp	1,620	quartz	10×6	1		364		
MJCV-5	385.25	Kp	Thp	182	no inclusion		0				

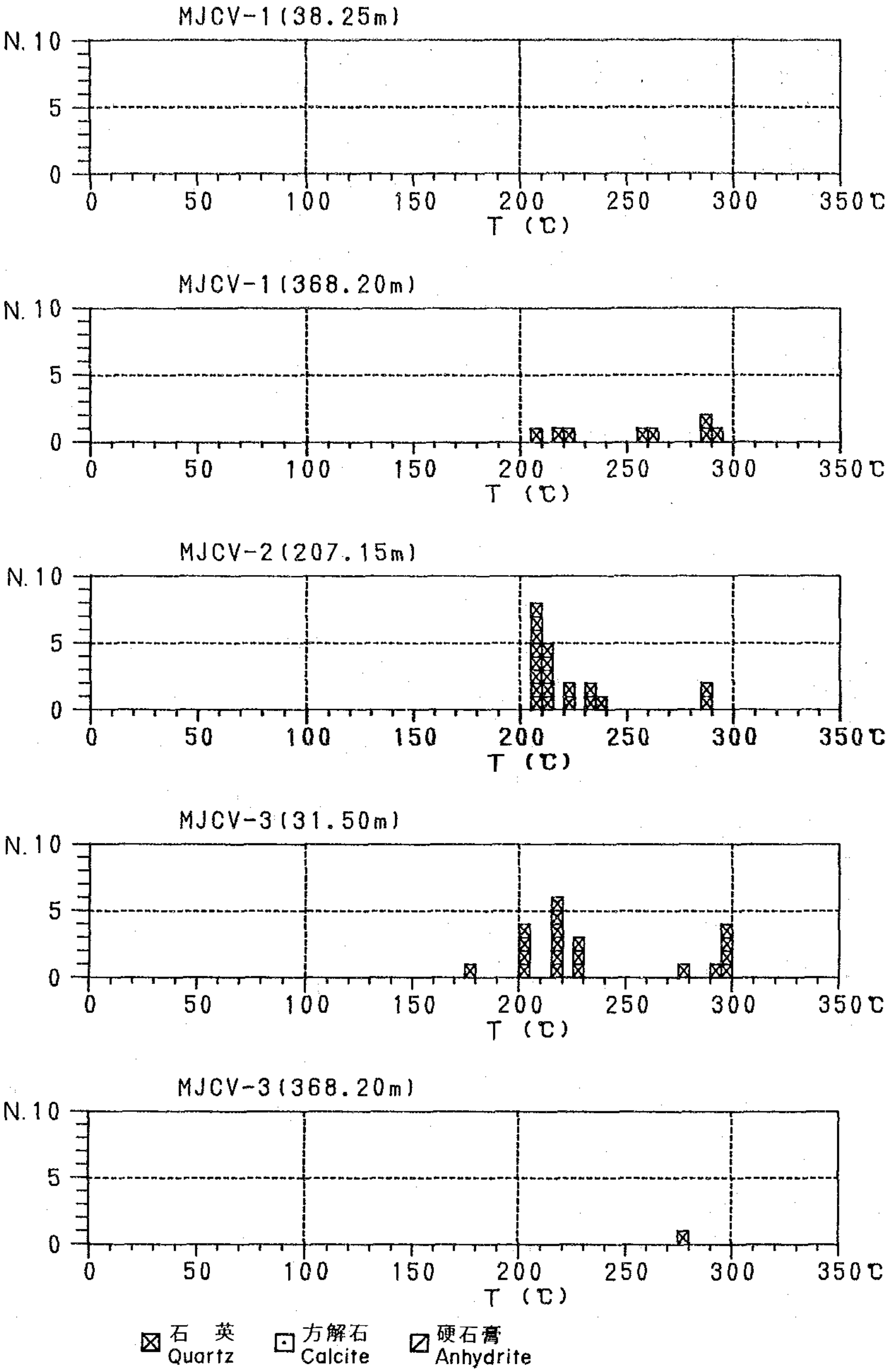

Fig.II-2-4 Distribution of homogenization temperature of fluid inclusion (1)

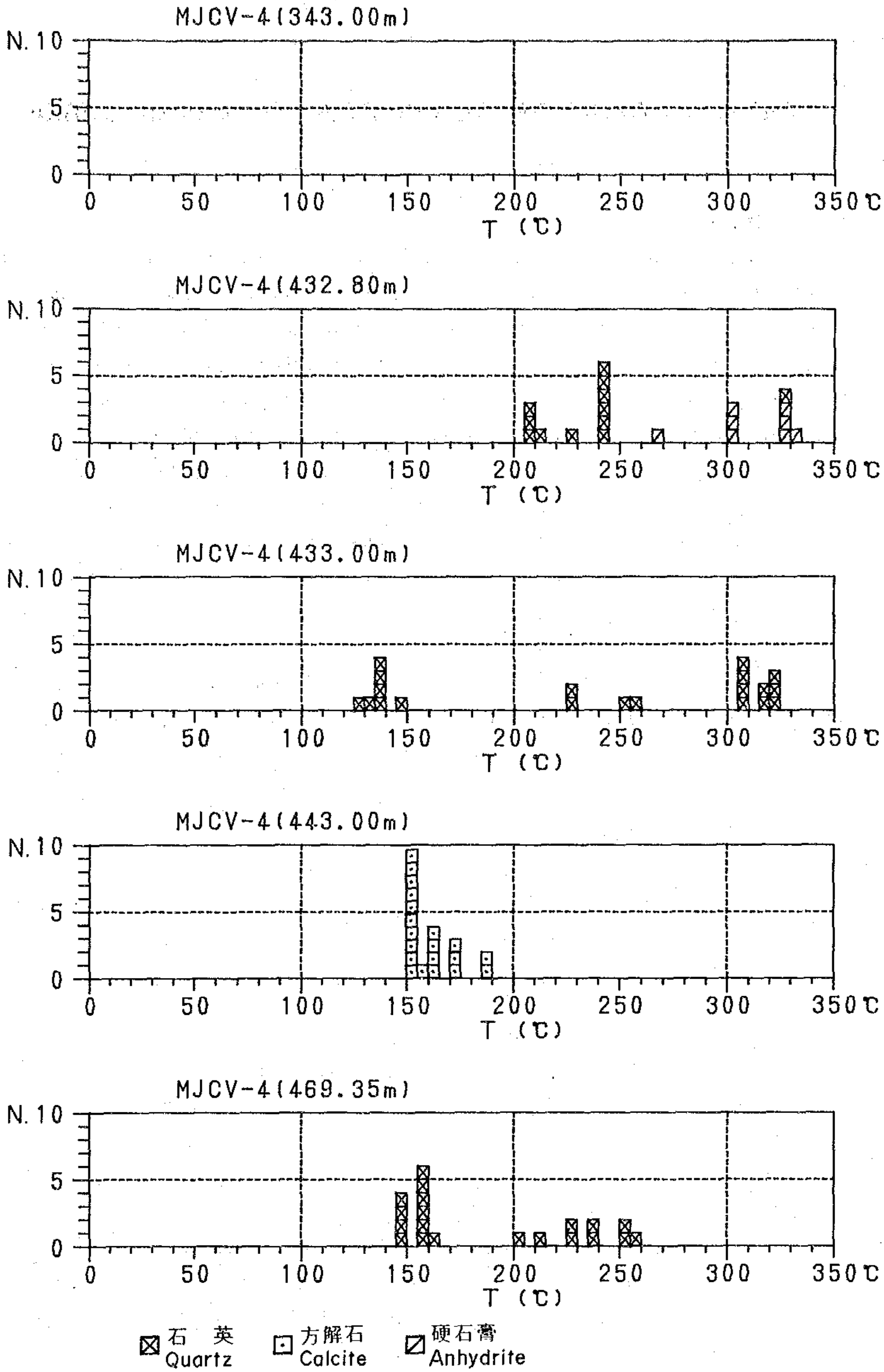

Fig.II-2-4 Distribution of homogenization temperature of fluid inclusion (2)

CHAPTER 3 GEOCHEMICAL SURVEY IN THE VERAGUAS AREA

3-1 Purpose

The survey is conducted in two methods; geochemical survey of caliche and rock. Caliche is the crust formed on the surface of the earth when salts dissolved in underground water rise to the surface through capillary action under dry climatic conditions where evaporation exceeds precipitation. It has been reported (Erickson and Marranzino, 1960) that in Utah, in the United States of America, marked anomalies in copper are observed in the caliche that cement to the pebbles close to the surface of the pebble stratum that covers the copper deposits over several tens of meters. This occurs under dry climatic conditions when mineral deposits exist below alluvium and colluvium; metal elements are carried to the surface by the evaporation of moisture and are fixed in the caliche. Thus it may be considered that geochemical anomalies in the caliche suggest the existence of mineral deposits beneath alluvium and colluvium. For this reason a geochemical survey was applied to the caliche in the areas of alluvium and colluvium in the survey area, the aim being to confirm the effectiveness of this method and to pinpoint new areas with prospective mineral deposits.

The geochemical survey of rock was done in the hilly area affected by mainly silicification in the southeast part of the survey area. Since this alteration zone is located in isolation on the outskirts of the survey area, no basic survey has been carried out systematically by ENAMI. Thus a geochemical survey of rock was carried out in order to understand the nature of the alteration zone and to study its relationship with the mineralization.

3-2 Survey Method

3-2-1 Sampling method

The areas of sizable distribution of caliche are the east and west parts of the San Juan to Veraguas hills, and these are the Pampa and Northwest districts where the samples of caliche were collected. Samples of rock were collected in the Pampa South district, southeast part of the survey area where the hills affected by alteration. (See Fig. 1) A location map of the sampling points is given in Fig. 2.

104 samples of caliche were collected from the Pampa District and 75 from the Northwest District, making a total of 179 samples. 49 samples of rock were collected from the Pampa South District and 2 from the San Juan Mine, making a total of 51 samples.

For the caliche, sampling lines were drawn up east to west, and samples were collected as a general rule at 200 metre intervals. As a general rule the sampling lines were spaced 500 metres apart in the Pampa District and 400 metres apart in the Northwest District. Where there was no caliche at a scheduled

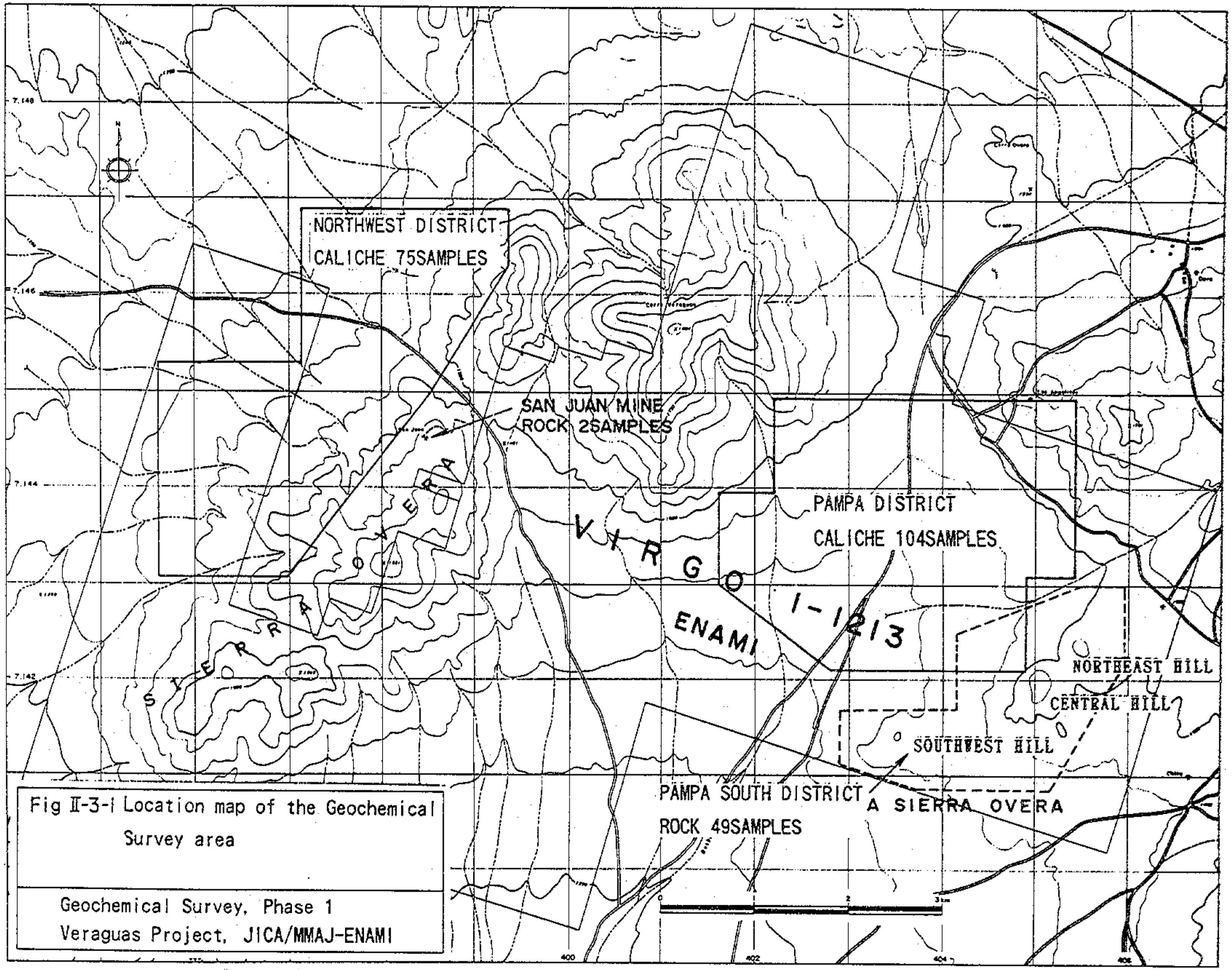

Fig II-3-1 Location map of the Geochemical Survey area

Geochemical Survey, Phase 1
Veraguas Project, JICA/MMAJ-ENAMI

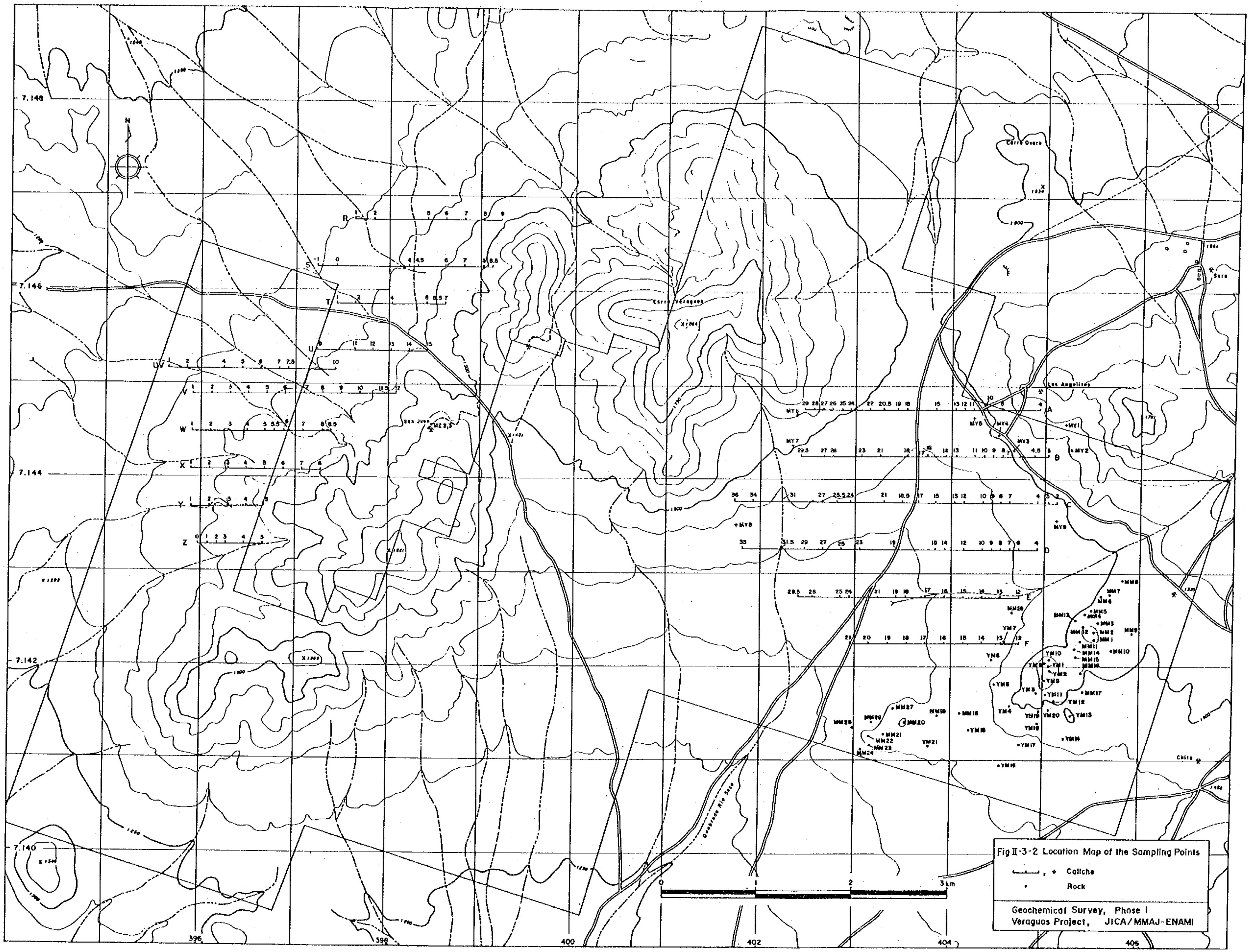

Fig II-3-2 Location Map of the Sampling Points

Geochemical Survey, Phase I
Veraguas Project, JICA/MMAJ-ENAMI

sampling point, but one of the pits known as Cata existed nearby and caliche was found either at the bottom of the pit or in dugout earth, this was taken as the sample. The size of each sample was roughly 200g. Where the caliche contained pieces of rock fragment, the rock fragment was as far as possible removed.

Rock samples were collected at intervals of 100 to 400 metres, keeping the sampling points as evenly spaced as possible. Samples were broken up in the field, and pieces with a minimum of weathered surface were taken. The size of each sample was roughly 200gm.

3-2-2 Chemical analysis and powder X-ray diffraction

Chemical analysis of the 179 samples of caliche and 51 samples of rock was carried out. The work was performed by the Chilean analysts, CESMEC LTDA. Components analyzed, detection limits and analytical methods, are as shown in Table 1.

In addition, powder X-ray diffraction was carried out on 10 representative samples of caliche in order to determine the variety of minerals. X-ray diffraction was also carried out on the 51 samples of rock to determine the alteration characteristic. The work was carried out at the Mitaka R&D Center of Nittetsu Mining Ltd.

3-3 Result of Survey

3-3-1 Geochemical survey of caliche

1. Statistical treatment of chemical analysis values

Table 2 shows the statistical parameters for the chemical analysis values, and Table 3 shows the correlation matrix. In the matrix it is characteristic that SiO_2, Fe_2O_3 and Cl show a mutually positive correlation, while this group shows a negative correlation with S. Concerning Cu, the largest correlation coefficient is 0.384033 between T.Cu and S.Cu, any significant correlation is not indicated with other chemical components, it may be considered that the behavior of Cu is independent of the behavior of the other chemical components. This suggests that the concentration of Cu is not carried out selectively in the salts of specific chemical components, but that the concentration of Cu in caliche is owing to the existence of mineral deposits.

In the statistical parameters (Table 2), values greater than the average value + standard deviation were taken to be geochemical anomalies, and where two or more geochemical anomalies occurred adjacent on the sampling line, this was considered to be a geochemical anomaly area. However, the following three instances were considered exceptions.

*Exception 1 : Where the distance between two adjacent points of geochemical anomaly was 300m or more, this was not considered a geochemical anomaly area.

*Exception 2 : Where a supplementary sample taken from between the sampling lines showed a geochemical anomaly, and the distance between this sample and one or more

Table II-3-1 Analytical method and detectable limits of the chemical analysis

Component	Detection limit	Analytical method
Cl	0.1 %	Volumetric
CO2	0.1 %	Combution
T.Cu	10 ppm	Atomic Absorption
S.Cu	10 ppm	Atomic Absorption
SiO2	0.2 %	Fusion-Gravimetry
FeO	0.05%	Volumetric
Fe2O3	0.05%	Atomic Absorption
S	0.1 %	Fusion-Gravimetry
SO4	0.1 %	Leaching-Gravimetry

Table II-3-2 Statistical parameter of caliche geochemistry (179 samples)

	Geometric average	Standard deviation	$M + 1/2\sigma$	$M + \sigma$
Cl	0.11%	0.53240	0.20%	0.38%
CO_2	0.15%	0.37805	0.23%	0.36%
T. Cu	38 ppm	0.94490	112 ppm	333 ppm
S. Cu	15 ppm	0.38351	24 ppm	37 ppm
SiO_2	20.1 %	0.21363	25.7 %	32.8 %
FeO	0.26%	0.35927	0.39%	0.59%
Fe_2O_3	1.16%	0.48181	2.03%	3.53%
S	10.5 %	0.27661	14.4 %	19.8 %
SO_4	9.3 %	0.22046	12.1 %	15.5 %

M : Geometric average

σ : Standard deviation (logrithm)

Table II-3-3 Matrix of the correlation coefficients of caliche geochemistry (179samples)

	Cl	CO2	Cu(total)	Cu(soluble)	SiO2	FeO	Fe2O3	S	SO4
Cl	1.000000								
CO2	-0.274130	1.000000							
Cu(total)	0.034167	0.021159	1.000000						
Cu(soluble)	-0.064651	0.252002	0.384033	1.000000					
SiO2	0.444277	-0.460078	0.028721	-0.152339	1.000000				
FeO	-0.566777	0.275972	-0.026804	0.086318	-0.092928	1.000000			
Fe2O3	0.442740	-0.416133	0.120085	0.061605	0.762872	-0.207961	1.000000		
S	-0.555028	0.401023	-0.107414	0.044791	-0.782289	0.344057	-0.647946	1.000000	
SO4	-0.296923	0.138774	-0.061406	0.039615	-0.413341	0.233086	-0.329591	0.731009	1.000000

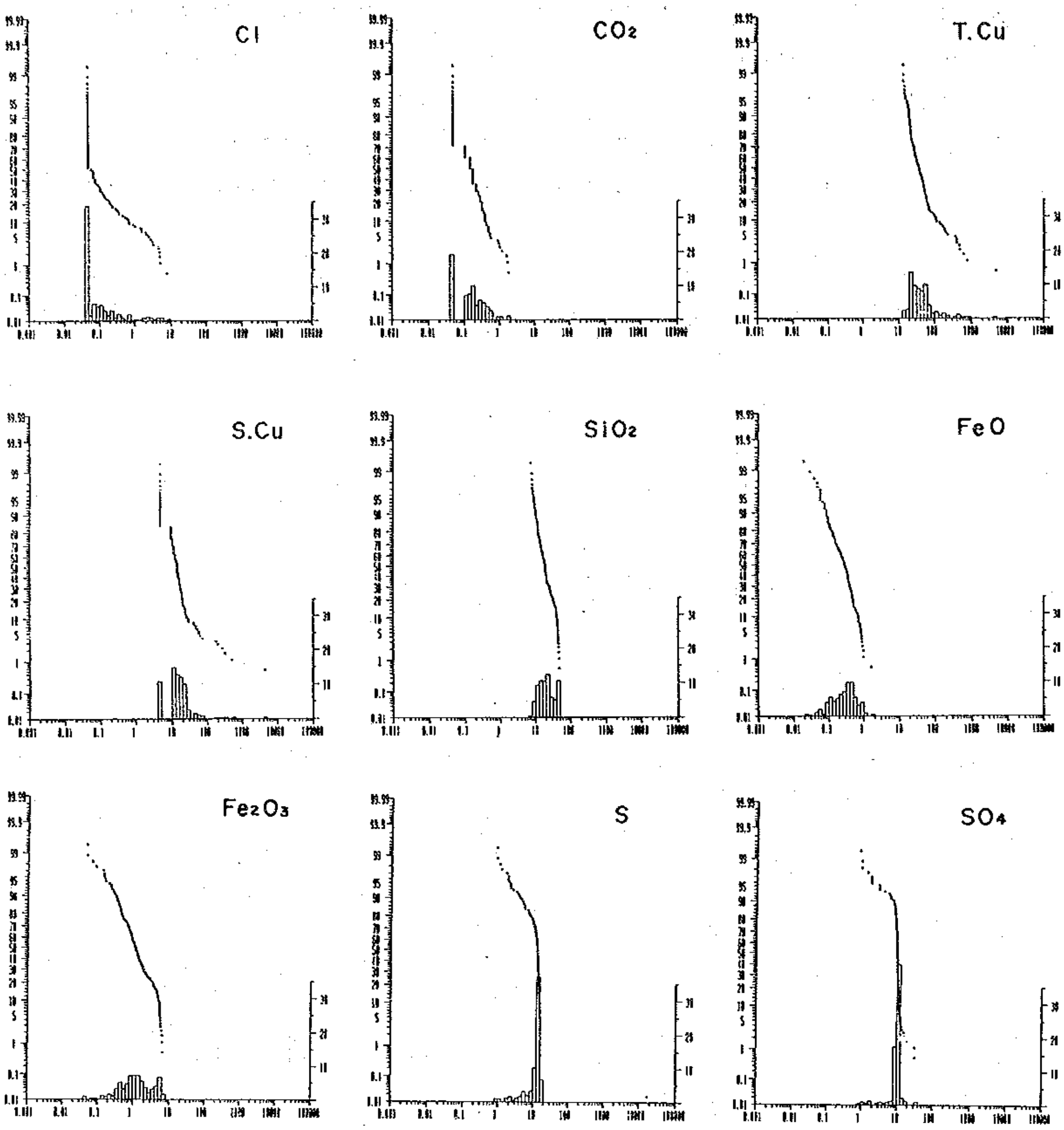

Fig II-3-3 Frequency distribution and cumulative distribution of the chemical analysis results of caliche samples taken on the sampling line showing geochemical anomaly was less than 300m, this was treated as a geochemical anomaly area.

*Exception 3 : In the case of S, there were no samples showing values greater than the average value + standard deviation, and so values greater than the average value + 2/3 standard deviation were taken to be geochemical anomalies.

In the case of S, as the histogram in Fig. 3 shows, there is a large dispersion in the lower chemical analysis values, so that no samples exist that show a value greater than average value + standard deviation.

The geochemical anomalies for each component and the geochemical anomaly area for the Pampa District and the Northwest District are shown in Figs. 4 to 15. Samples of T.Cu and S.Cu showing values greater than the average value + 1/2 standard deviation are also shown for reference.

2. Geochemical anomalies in the Pampa District

T.Cu: Four points of geochemical anomaly exist around the Pampa Mine, and 2 samples in just vicinity of the mine form a geochemical anomaly area. Six samples showing values greater than average values + 1/2 standard deviation are also distributed around the Pampa Mine.

S.Cu: A geochemical anomaly area consisting of 8 samples is formed around the Pampa Mine. Of 10 samples showing values greater than average values + 1/2 standard deviation, 6 are distributed around the geochemical anomaly area.

FeO: Geochemical anomalies exist from the Pampa Mine towards the SSW of the area, and a geochemical anomaly area is formed on sampling line D. Geochemical anomalies are also scattered in the western part of the district, and in general there is a tendency for anomaly to occur in NNW/SSE trend.

Fe_2O_3: Near to the Pampa Mine, one sample shows geochemical anomaly. Geochemical anomalies are also observed scattering around the western part of the district. A geochemical anomaly area comprising 2 samples exists in the SW part of the area. Only one sample overlaps with anomaly in FeO.

S: Two geochemical anomaly areas, each comprised of 2 samples, and scattered 6 samples showing geochemical anomaly, exist around the Pampa Mine. On the west side of sampling line A also, there exist 4 samples showing geochemical anomaly.

SO_4: One sample showing geochemical anomaly exists on sampling line D, roughly in the center of the district. This does not overlap with the geochemical anomalies of S.

SiO_2: 10 samples showing geochemical anomaly are scattered, all but one being in the west part of the district.

CO_2: Scattered points of geochemical anomaly and three geochemical anomaly areas, each comprising two samples, occurred around and to the south of the Pampa Mine.

Cl: Points of geochemical anomaly are scattered through the SW part of the district. There are also 2 samples of geochemical anomaly on sampling line A.

3. Geochemical anomalies in the Northwest District

T.Cu: There is a geochemical anomaly area comprising two samples on sampling line W. Nearby are three samples showing values greater than the average value + 1/2 standard deviation.

S.Cu: There is a geochemical anomaly area comprising three samples on sampling line W. This includes the geochemical anomaly area of T.Cu . Nearby are two samples showing values greater than the average value + 1/2 standard deviation.

FeO: Geochemical anomaly areas occur in two places along sampling line W. The geochemical anomaly area comprising three samples located toward the east duplicates the geochemical anomaly area of S.Cu.

Fe_2O_3: Geochemical anomaly areas are distributed in 5 places. Of these, the areas on sampling lines S and T, sampling lines V, W and X, and sampling lines Y and Z, show a large area of distribution. The geochemical anomaly area comprised of 10 samples on sampling lines V, W and X includes two samples that overlap anomalies of T.Cu, S.Cu and FeO.

S: There is a geochemical anomaly area comprising two samples on sampling line X.

SO_4: Four samples in the north part of the district show geochemical anomaly. Of these, the two samples on sampling line T form a geochemical anomaly area. This does not overlap the anomalies of S.

SiO_2: Relatively large geochemical anomaly areas occur in three places. These harmonize well with the distribution of geochemical anomalies of Fe_2O_3 .

CO_2: There are two geochemical anomaly areas. Of these the geochemical anomaly area on sampling line W includes the distribution of a geochemical anomaly area of FeO.

Cl: There are three geochemical anomaly areas, each comprising two samples. Of these, the areas on sampling line S and sampling line Z are included in geochemical anomaly area of SiO_2 and Fe_2O_3.

4. Results of powder X-ray diffraction

As a result of powder X-ray diffraction carried out on 10 representative samples (Table 7), gypsum was detected in 9 samples; albite in 8 samples; and quartz in 7 samples. It was ascertained that caliche is basically made up of gypsum, albite and quartz. Other minerals detected were one instance each of niter, halite and sepiolite.

3-3-2 Geochemical survey of rock

1. Statistical treatment of chemical analysis values

Table 4 shows the statistical parameters for the chemical analysis values, and Table 5 shows the correlation matrix. Noteworthy character in the statistical parameters is that the average value of SiO_2 is

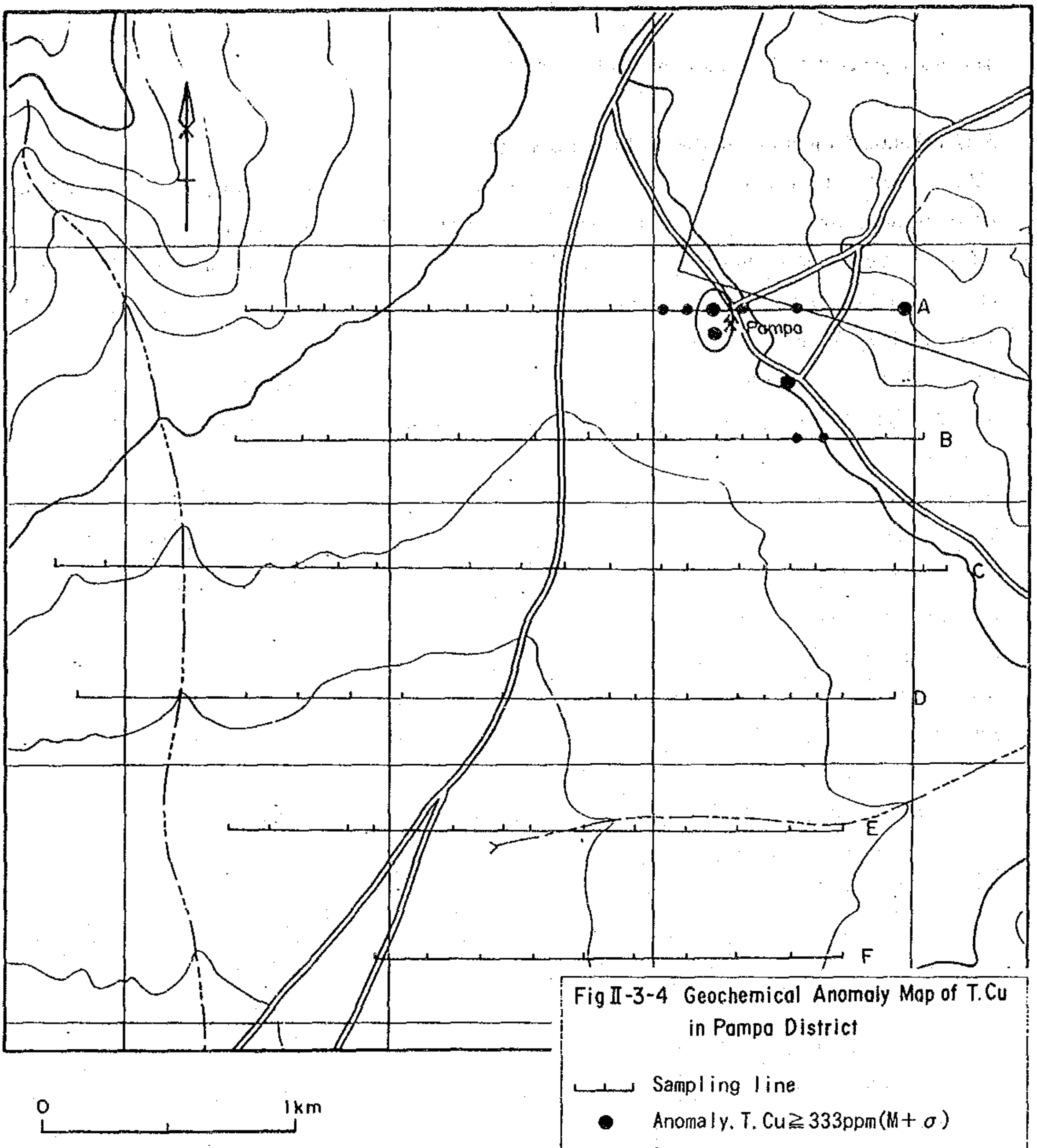

Fig II-3-4 Geochemical Anomaly Map of T.Cu in Pampa District

Sampling line

Anomaly, T.Cu≧333ppm(M+σ)

Subanomaly, 333ppm>T.Cu≧112ppm(M+1/2σ)

Anomaly area of T.Cu

M:Geometric average

σ:Standard deviation

Geochemical Survey, Phase 1
Veraguas Project, JICA/MMAJ-ENAMI

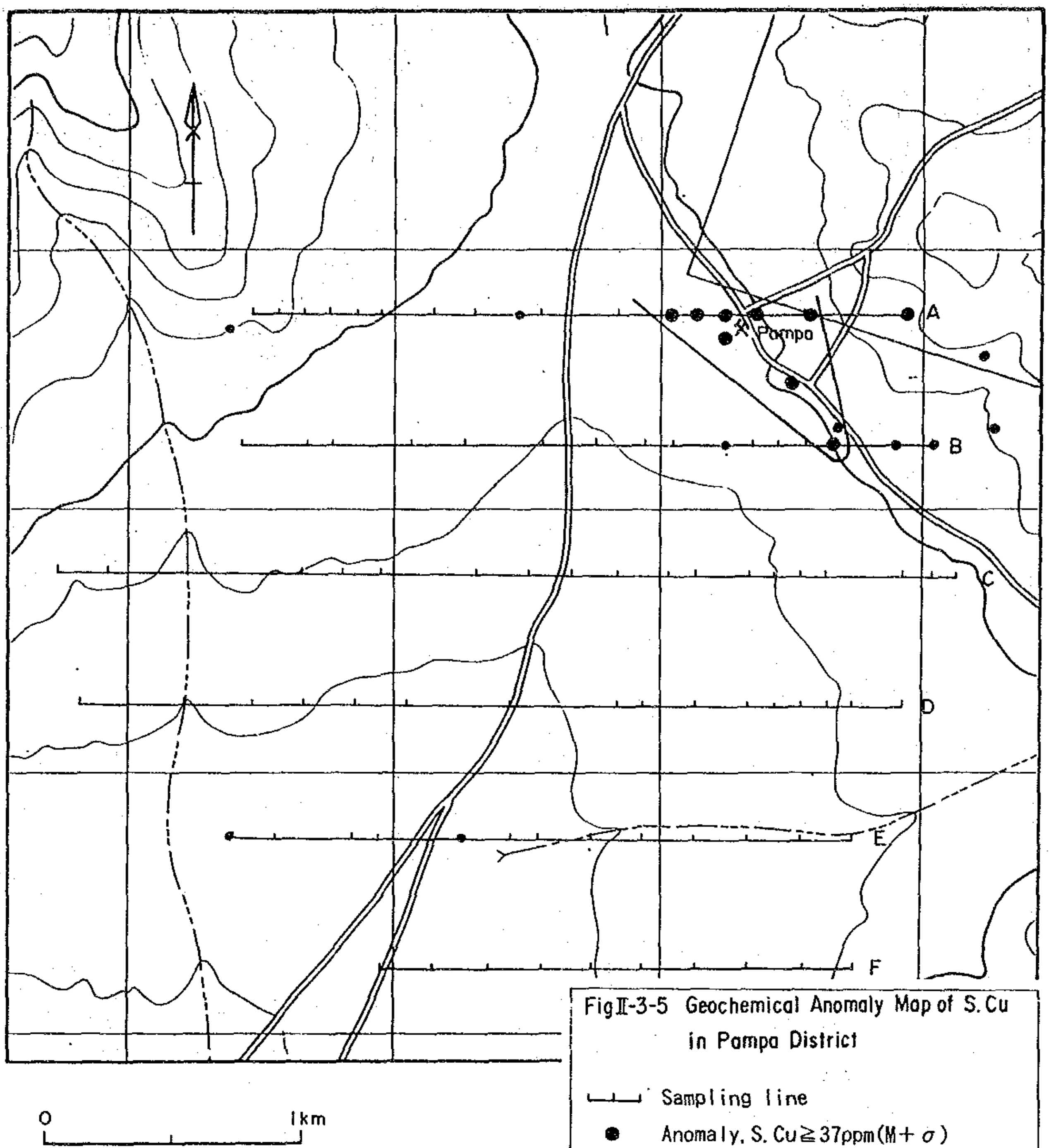

Fig II-3-5 Geochemical Anomaly Map of S.Cu in Pampa District

Sampling line
Anomaly, S.Cu≧37ppm(M+σ)
Subanomaly, 37ppm>S.Cu ≧24ppm(M+1/2σ)
Anomaly area of S.Cu

M:Geometric average
σ:Standard deviation

Geochemical Survey, Phase 1
Veraguas Project, JICA/MMAJ-ENAMI

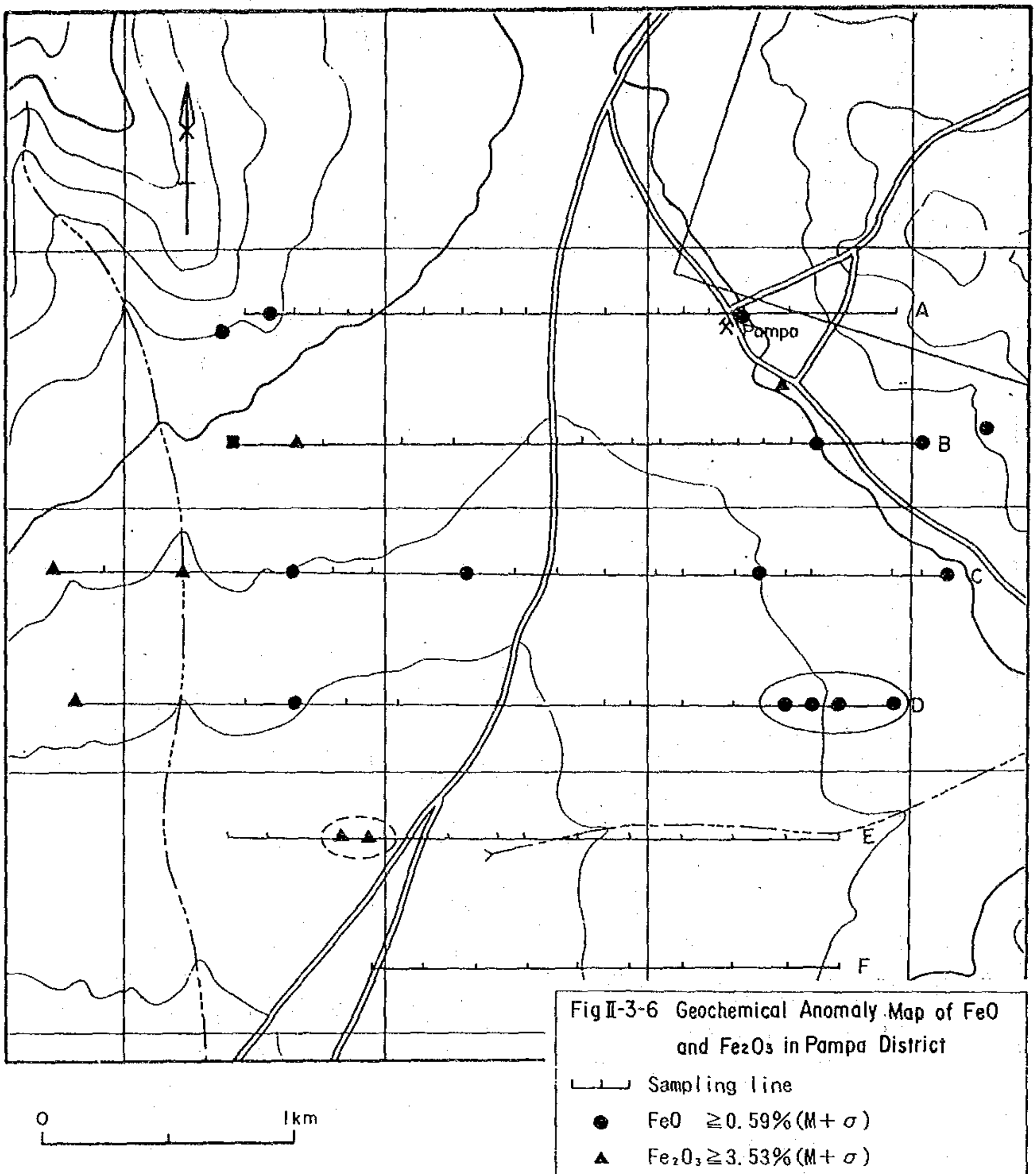

Fig II-3-6 Geochemical Anomaly Map of FeO and Fe_2O_3 in Pampa District

Sampling line
● FeO ≧0.59%(M+σ)
▲ Fe_2O_3≧3.53%(M+σ)
■ FeO and Fe_2O_3
Anomaly area of FeO
Anomaly area of Fe_2O_3
M:Geometric average
σ:Standard deviation

Geochemical Survey, Phase 1
Veraguas Project, JICA/MMAJ-ENAMI

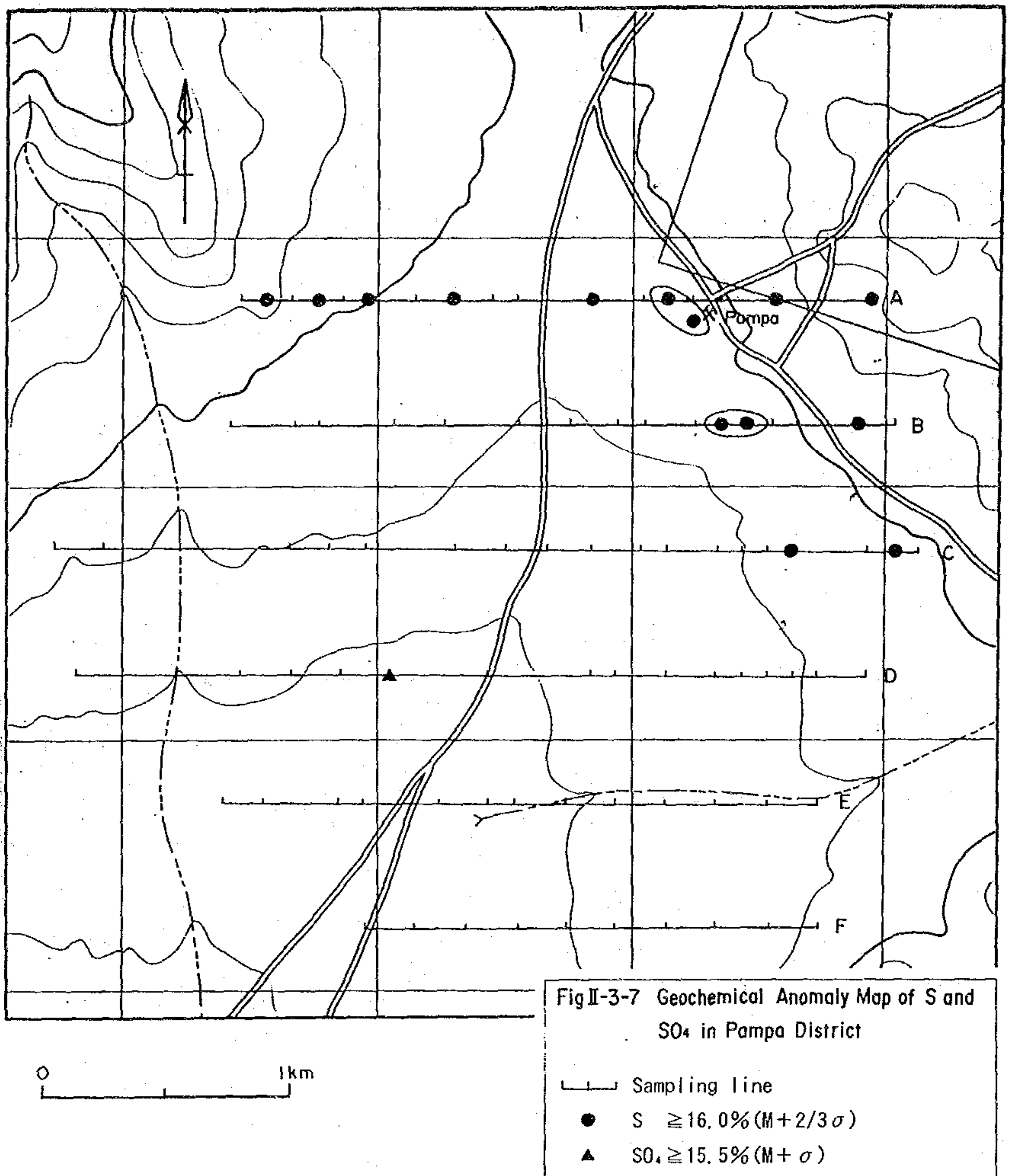

Fig II-3-7 Geochemical Anomaly Map of S and SO_4 in Pampa District

Sampling line

● S ≧16.0%(M+2/3σ)

▲ SO_4≧15.5%(M+σ)

Anomaly area of S

M:Geometric average

σ:Standard deviation

Geochemical Survey, Phase 1
Veraguas Project, JICA/MMAJ-ENAMI

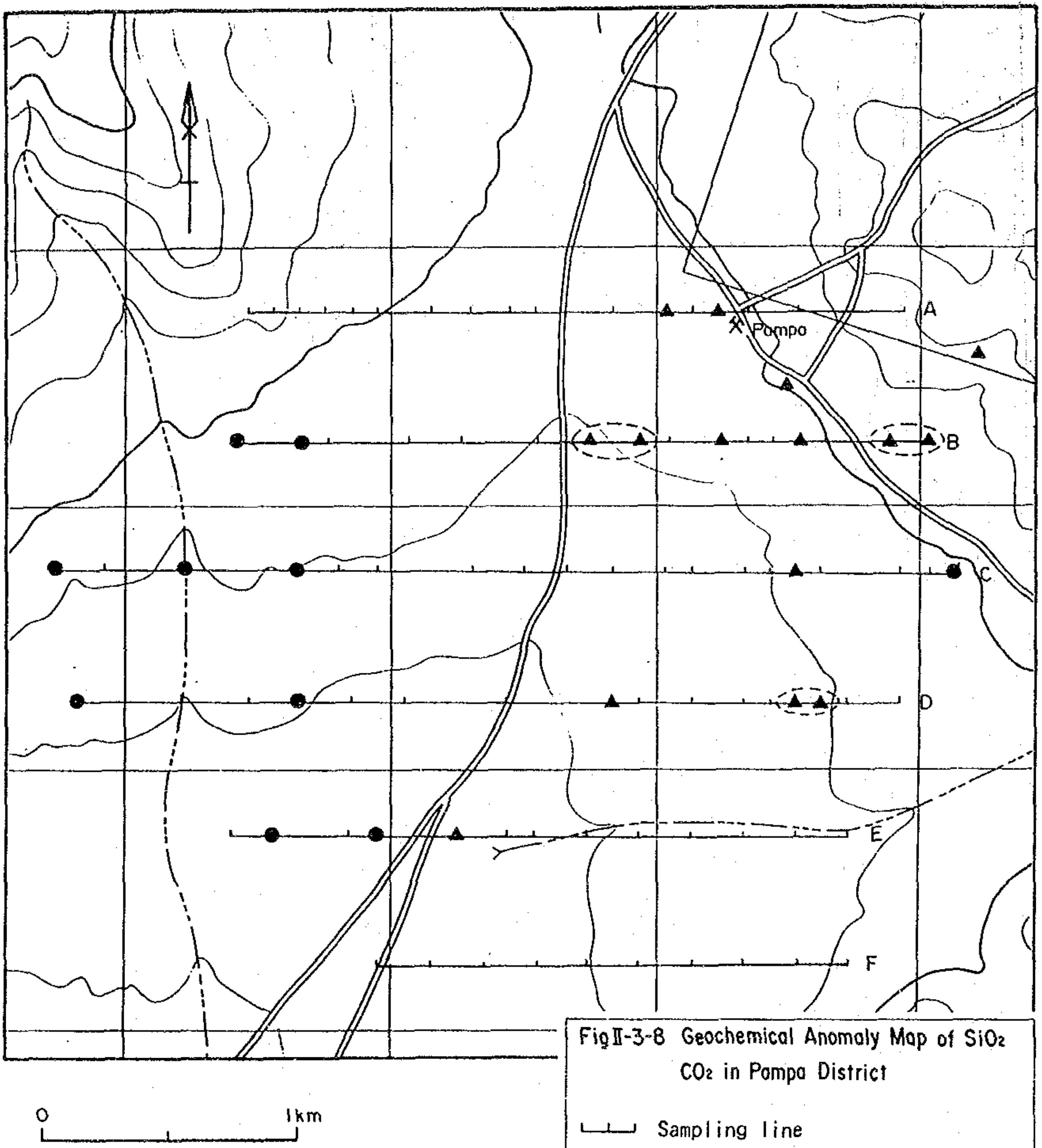

Fig II-3-8 Geochemical Anomaly Map of SiO_2 CO_2 in Pampa District

Sampling line

● $SiO_2 \geqq 32.8\%$ $(M+\sigma)$

▲ CO_2 $\geqq 0.36\%$ $(M+\sigma)$

Anomaly area of CO_2

M:Geometric average

σ :Standard deviation

Geochemical Survey, Phase 1
Veraguas Project, JICA/MMAJ-ENAMI

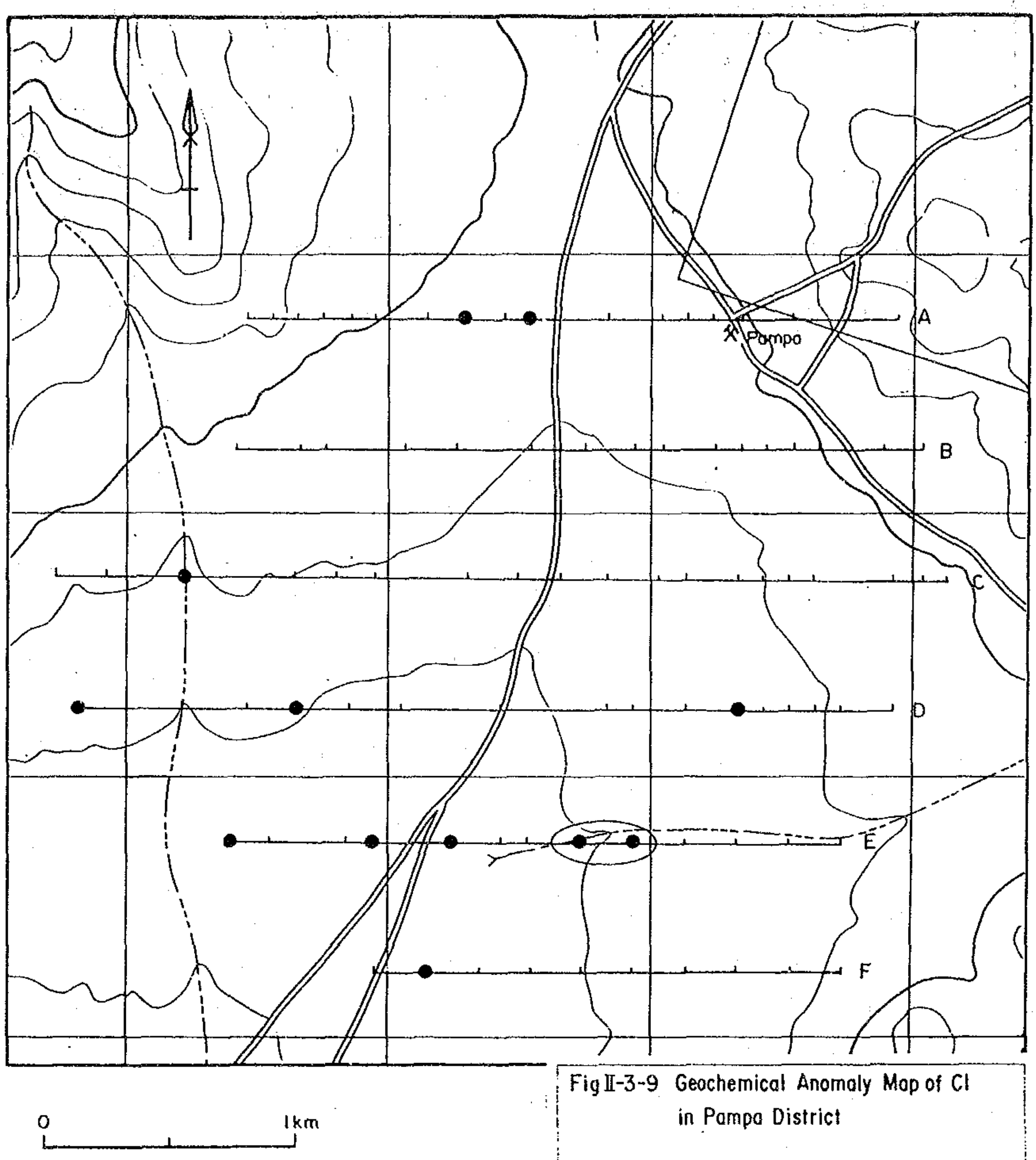

Fig II-3-9 Geochemical Anomaly Map of Cl in Pampa District

Sampling line
● Cl ≧ 0.38% (M + σ)
Anomaly area of Cl

M: Geometric average
σ: Standard deviation

Geochemical Survey, Phase 1
Veraguas Project, JICA/MMAJ-ENAMI

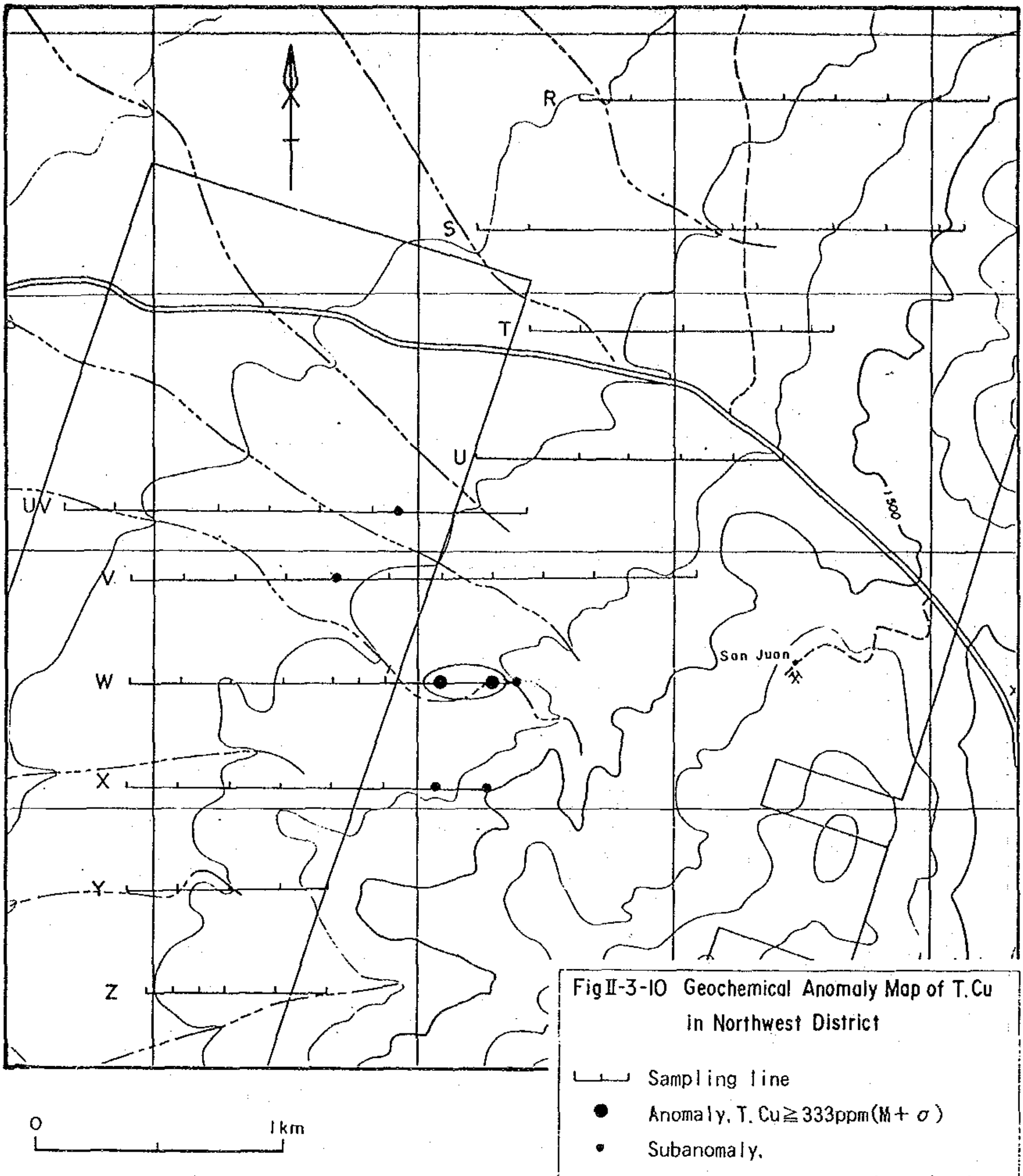

Fig II-3-10 Geochemical Anomaly Map of T.Cu in Northwest District

Sampling line
Anomaly, T.Cu ≧ 333ppm (M + σ)
Subanomaly, 333ppm > T.Cu ≧ 112ppm (M + 1/2 σ)
Anomaly area of T.Cu

M: Geometric average
σ: Standard deviation

Geochemical Survey, Phase 1
Veraguas Project, JICA/MMAJ-ENAMI

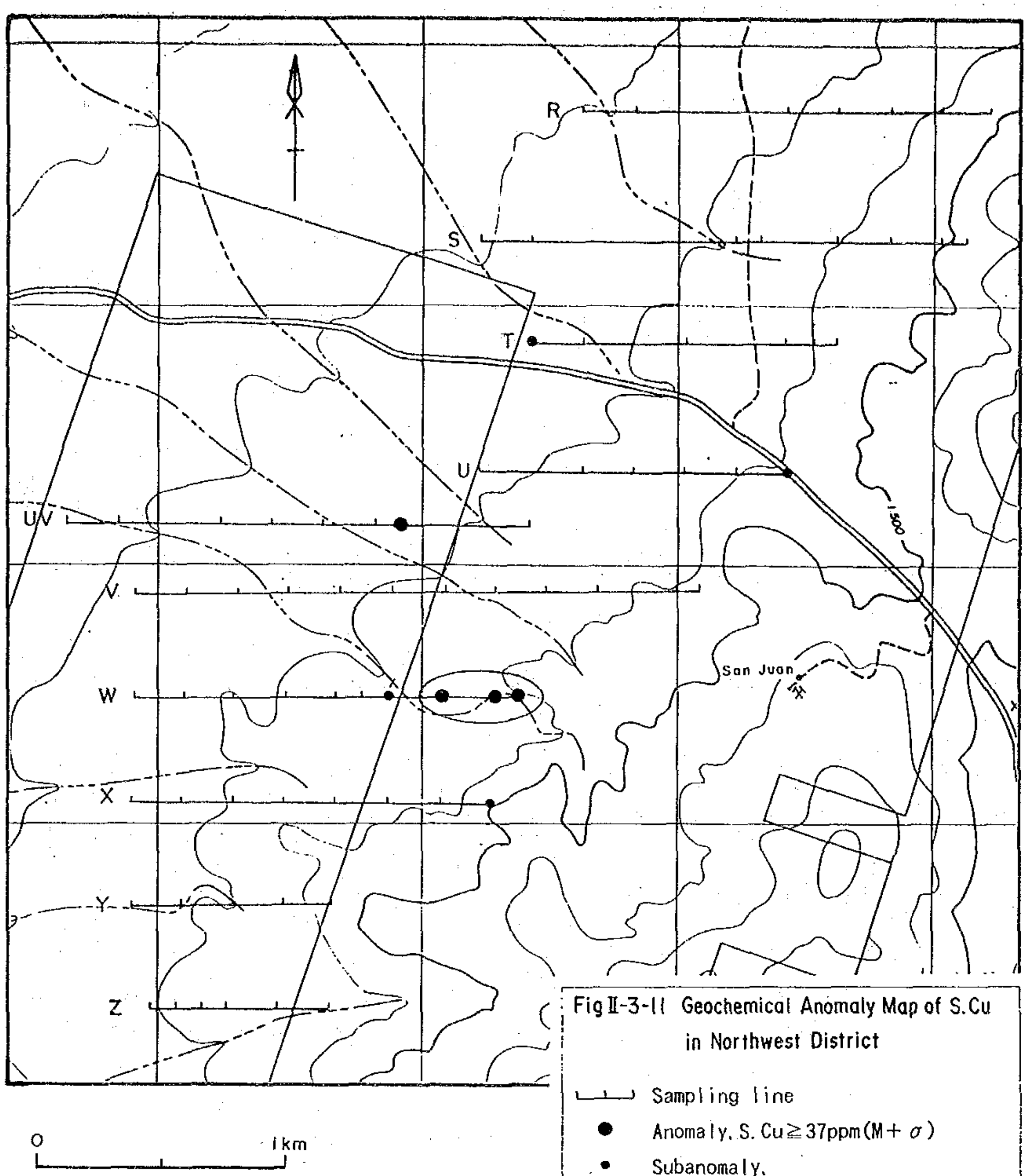

Fig II-3-11 Geochemical Anomaly Map of S.Cu
in Northwest District

- Sampling line
- ● Anomaly, S.Cu≧37ppm(M+σ)
- • Subanomaly, 37ppm >S.Cu≧24ppm(M+1/2σ)
- ⬭ Anomaly area of S.Cu

M:Geometric average
σ :Standard deviation

Geochemical Survey, Phase 1
Veraguas Project, JICA/MMAJ-ENAMI

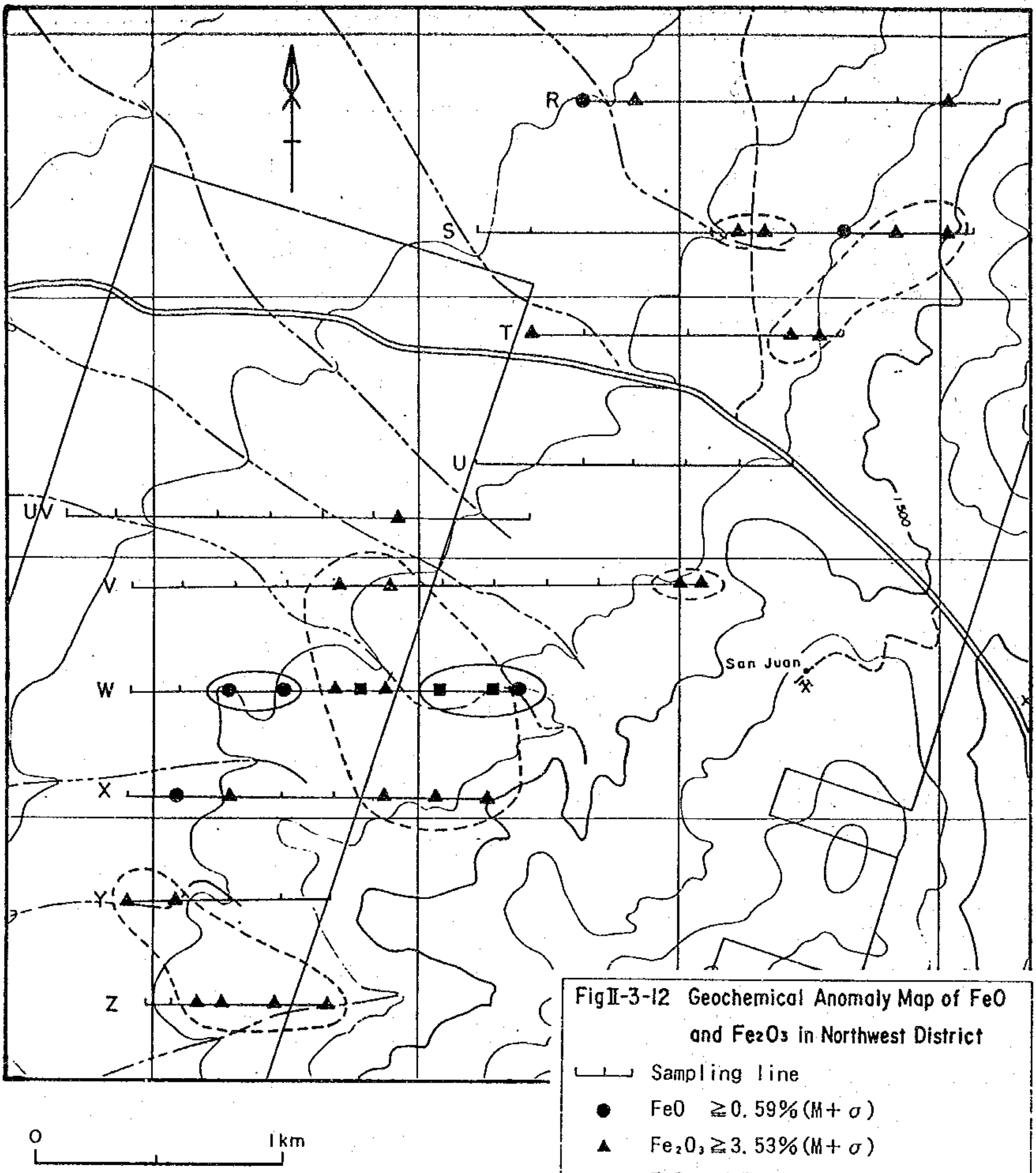

FigⅡ-3-12 Geochemical Anomaly Map of FeO and Fe_2O_3 in Northwest District

- Sampling line
- ● FeO ≧0.59%(M+σ)
- ▲ Fe_2O_3 ≧3.53%(M+σ)
- ■ FeO and Fe_2O_3
- Anomaly area of FeO
- Anomaly area of Fe_2O_3

M:Geometric average

σ:Standard deviation

Geochemical Survey, Phase 1
Veraguas Project. JICA/MMAJ-ENAMI

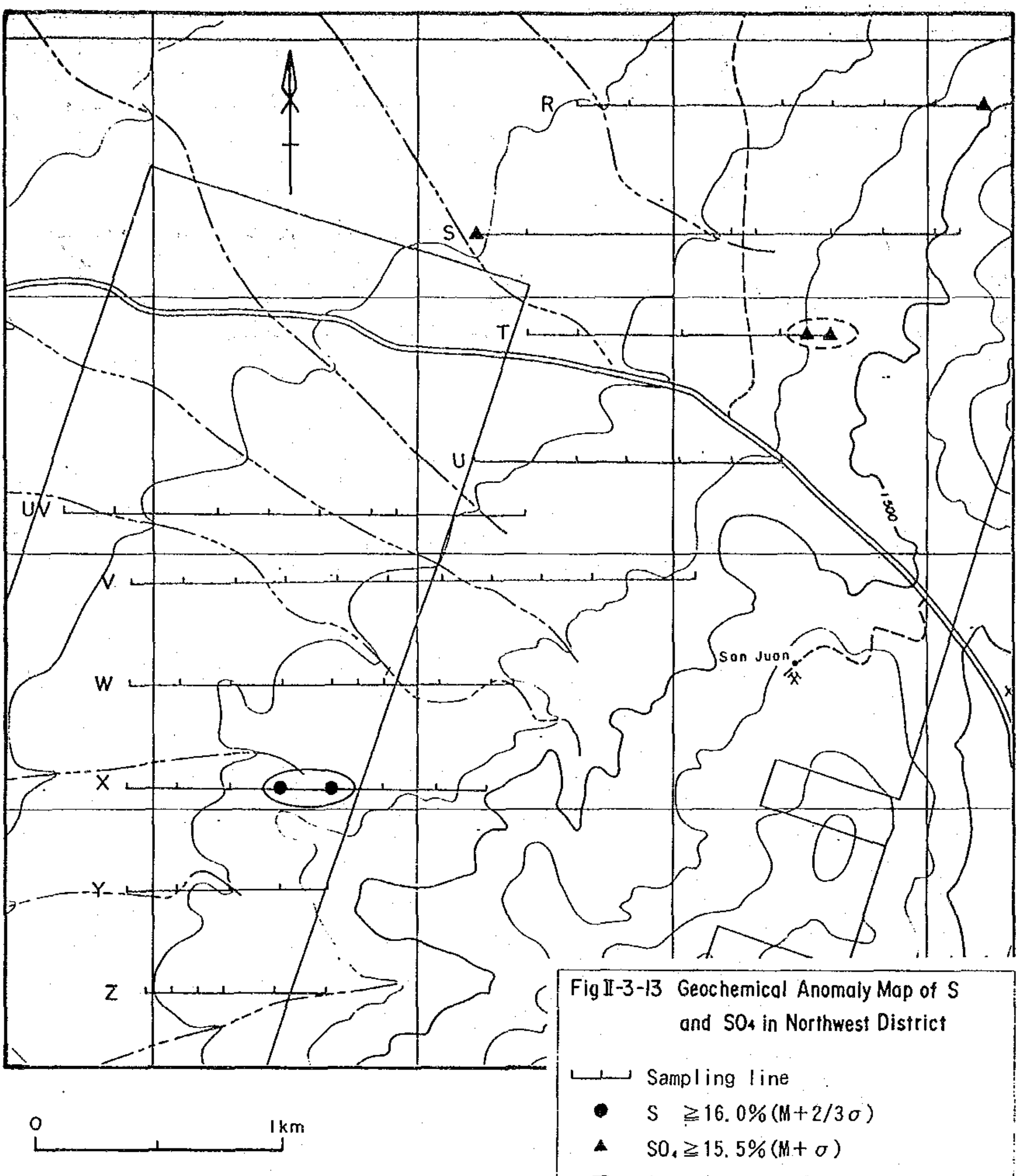

Fig II-3-13 Geochemical Anomaly Map of S and SO_4 in Northwest District

Sampling line
● S ≧16.0%(M+2/3σ)
▲ SO_4 ≧15.5%(M+σ)
Anomaly area of S
Anomaly area of SO_4

M:Geometric average
σ:Standard deviation

Geochemical Survey, Phase 1
Veraguas Project, JICA/MMAJ-ENAMI

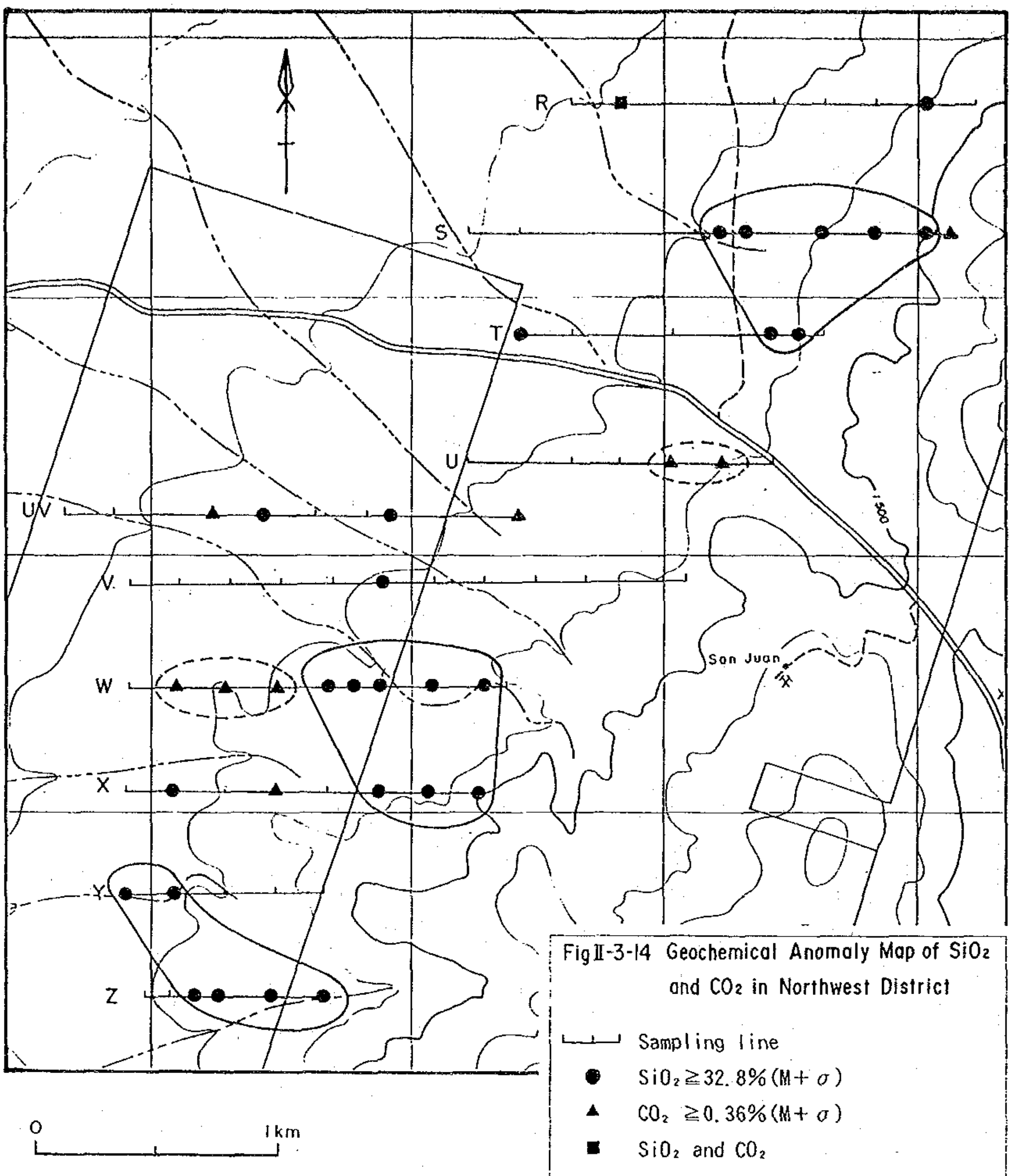

Fig II-3-14 Geochemical Anomaly Map of SiO_2 and CO_2 in Northwest District

- Sampling line
- ● $SiO_2 \geqq 32.8\% (M+\sigma)$
- ▲ $CO_2 \geqq 0.36\% (M+\sigma)$
- ■ SiO_2 and CO_2
- Anomaly area of SiO_2 (solid outline)
- Anomaly area of CO_2 (dashed outline)

M: Geometric average

σ: Standard deviation

Geochemical Survey, Phase 1
Veraguas Project, JICA/MMAJ-ENAMI

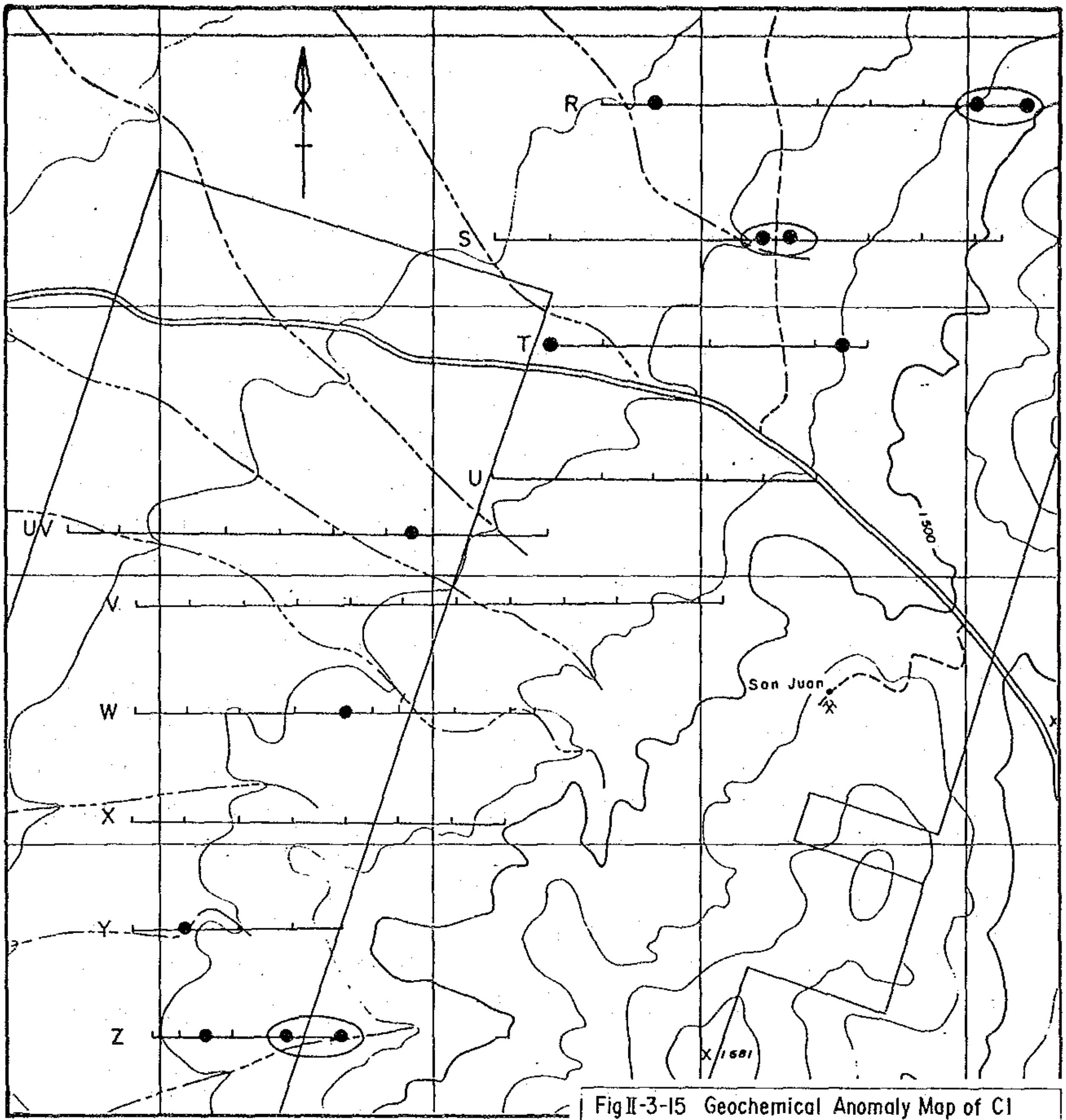

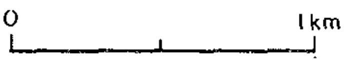

Fig II-3-15 Geochemical Anomaly Map of Cl in Northwest District

Sampling line
● Cl ≧ 0.38% (M + σ)
Anomaly area of Cl

M: Geometric average
σ: Standard deviation

Geochemical Survey, Phase 1
Veraguas Project, JICA/MMAJ-ENAMI

48.7wt%. The rock from which samples were taken are altered rocks that were originally volcanic rocks, and intrusive rock (Fig. 18); most of the altered rock can be seen by the naked eye to have undergone silicification or strong silicification, and it may be imagined that it underwent the addition of SiO_2 ; even so, an average value of 48.7% for SiO_2 suggests that the original rock was basaltic rocks. It is also characteristic that, while according to R.A. Daly (1933) in the average chemical composition of basalt the values for FeO and Fe_2O_3 are 6.37% and 5.38% respectively, the samples studied in the present survey show markedly low values, at 0.97% and 1.49% respectively. In the matrix the only combinations that show an absolute value of 0.5 or more are T.Cu-S.Cu and S-SO_4, where the chemical composition is similar. Although with absolute values of less than 0.5 the correlation is weak, it may be noted that S shows a negative correlation with T.Cu and Fe_2O_3 .

In the statistical parameters values greater than the average value + standard deviation were taken to be geochemical anomalies, and where two or more geochemical anomalies occurred adjacent to each other, this was considered to be a geochemical anomaly area. However, where the distance between such points was 500m or more, this was not considered a geochemical anomaly area.

Of the nine components that were subjected to chemical analysis, comment will be made on T.Cu, S, FeO and Fe_2O_3; the analytical values for the other components will merely be given in Table 8. The reason for this is that S.Cu shows a high positive correlation with T.Cu, and SO_4 (soluble S) shows a high positive correlation with S (total S), and the behavior of copper and sulfur can be represented by T.Cu and S. As for SiO_2 ,CO_2 and Cl, no geochemical anomalies worth commenting on were obtained. Geochemical anomalies and geochemical anomaly areas are shown on Figs. 19 and 20.

2. Geochemical anomalies

In describing geochemical anomalies, the three groups of hills running NE to SW which make up the area under discussion, will be called, from the NE, the Northeast Hill, Central Hill and Southwest Hill (Fig. 1).

T.Cu: 7 samples showed geochemical anomaly. Of these 4 samples are distributed on the northeast of the Northeast Hill, and here a geochemical anomaly area comprising 2 samples is formed. A geochemical anomaly area comprising 2 samples is also located between the Central Hill and Southwest Hill.

S: 3 samples showing geochemical anomaly occur around the summit of the Northeast Hill, and 2 of these forms geochemical anomaly area. Single samples of geochemical anomaly also occurs south of the Central Hill and southwest of the Southwest Hill.

FeO: A geochemical anomaly area comprising 3 samples is located on the northeast of the Northeast Hill. Of these 2 samples also show geochemical anomaly of T.Cu. There was also a geochemical anomaly area comprising 3 samples on the east of the Central Hill.

Fe_2O_3:A geochemical anomaly area comprising 2 samples is located on the east of the Southwest Hill,